02/10/94

Do Coronal Holes Cause 27 Day Recurring Geomagnetic Storms'?

Bruce T. Tsurutani[1]
Walter D. Gonzalez[2]
Alicia L. C. Gonzalez[2]
Frances Tang[3]
Dan Park [1]
Masaki Okada[4]
John Arballo[1]

[1]Jet Propulsion Laboratory,
California Institute of Technology,
Pasadena, California 91209

[2]Instituto National Pesquisas Espaciais (INPE),
Sao Jose dos Campos, Sao Paulo, Brazil

[3]California Institute of Technology
Pasadena, California 91125

[4]RASC, Kyoto University, Uji, Japan

Abstract

We examine 3 years of interplanetary data and geomagnetic activity indices (1973-1975) to determine. the causes of geomagnetic storms and substorms during the descending phase of the solar cycle. In this paper we specifically studied the year 1974 where two long lasting corotating streams existed. We find that major (Dst ≤ -100 nT) storms are caused by CMEs related to solar flares and not by the corotating streams from coronal holes. Because far fewer CMEs occur near solar minimum, there are only 3 such storms in 1974. Corotating streams can cause moderate (- 100 nT ≤ Dst ≤ -50 nT) to weak (-50 nT ≤ Dst ≤ -25 nT) recurring storms. The southward interplanetary magnetic fields that cause these geomagnetic storms occur at the region where the corotating stream interacts with the heliospheric current sheet (HCS) and its plasma sheet. A model for this interaction and the formation/enhancement of the plasma sheet is presented. It should be noted that corotating streams very often have little or no effect on the Earth's ring current (Dst ≥ -25 nT). Although high intensity magnetic fields (15-25 nT hourly average) are still generated at the corotating stream/HCS interaction region, in these cases there are no significant southward components to lead to intense reconnection events and magnetic storms. The most dramatic geomagnetic response to the corotating streams are continuous auroral activity called HILDCAAs. The continuous auroral substorm activity is caused by southward components of Alfvén waves. These waves are present throughout most of the stream. The start of the HILDCAAs begins with the stream onset and gradually fades away as the velocity of the stream and the Alfvén wave amplitudes decrease. These 27-day recurring events can last 10 days or more. This phenomenon dominates the Ap and Kp indices. 27 day recurring intervals of low AE (< 200 nT) and positive Dst intervals have also been identified. The former arc due to low intensity (radial) fields in the trailing portions of high speed streams and the latter are related to the passage of high plasma density regions near the heliospheric current sheet (HCS). A schematic illustrating the interplanetary regions causing storms, HILDCAAs, geomagnetic quiet and positive Dst storms is provided.

INTRODUCTION

Recently, there has been considerable attention focused on the interplanetary and solar causes of magnetic storms which have occurred at and near solar maximum (Gonzalez and Tsurutani, 1986; Burlaga et al., 1987; Tsurutani et al., 1987; Tang et al., 1989; Gonzalez et al., 1989; Hoeksema and Xu, 1991; Gosling et al. 1991; Tsurutani et al., 1992; Crooker et al., 1992; Gonzalez et al., 1993), It has been clearly demonstrated (Feynman and Gu, 1986) that during this phase of the solar cycle, the predominant type of solar events associated with high speed streams in interplanetary space are Coronal Mass Ejections or CMEs (Timothy et al., 1975, Gosling et al., 1991). It has recent] y been shown that CMEs sometimes occur slight] y before flares and prominence eruptions (Harrison, 1986; 199 1) and thus flares and prominence eruptions cannot be the cause of CMEs. It is most likely that there is some mechanism responsible for both flares/prominence eruptions and CMEs.

In 1940, Chapman and Bartel discussed storms which recur at 27 day intervals. Because there were no visible features "on the sun that were correlated with such storms (such as flares), they ascribed the solar source of the storms as activity at M (for mystery) regions. On the other hand, Coronal Mass ejections are impulsive events (Hundhausen, 1993) which occur at times when the instability criteria at helmet streamers are met (Wolf son et al., 1987; Low and Smith, 1993). One would therefore not expect this mechanism to cause storms at Earth with any regularity. Clearly, there must be another solar source for recurrent geomagnetic activity.

We now know that these M-regions must be coronal holes. During and near solar minimum, polar coronal holes can extend down to the equator and can remain there for duration of months or longer (Zirker, 1977). The high speed solar wind coming from these holes is emitted continuously and because the hole is (relatively) fixed at the Sun, the high speed stream "corotates" with the Sun's rotational period. Thus, if the hole extends to the ecliptic plane, the corotating stream engulfs the Earth's magnetosphere once every 27 days.

It is one of the purposes of this paper to examine the geoeffectiveness of high speed corotating streams emanating from coronal holes. Clearly, features of corotating streams leading to geomagnetic storms at Earth may be substantially different from those for CMEs. As one major example, one would not expect the presence of intense magnetic clouds with large north-south orientations (Klein and Burlaga, 1982, Ferrugia et al. 1993) to be present in the corotating streams. During and near solar maximum, magnetic clouds are the source of approximately half of the intense B_S events which cause intense and great storms (Tsurutani et al., 1988; 1992). Also, because the plasma is continuously (not impulsively) ejected from coronal holes, fast forward shocks can only form at the corotational interface (see figure in Tsurutani et al., 1982).

Typically shocks at the corotating stream interface arc not thought to form until distances greater than - 1.5 AU from the Sun (Smith and Wolfe, 1993). Thus, without strong shock compression of the interplanetary magnetic fields, one might expect lower IMF magnitudes, lower intensity B_Z components, and therefore weaker geomagnetic activity. However, it has been noted (Saba, 1992) that the average AE for 1974 was higher than that for 1979, a solar maximum year where these were numerous and very large magnetic storms. This feature will be addressed and explained as WC]].

We will also address the commonly held notion that there are 27 day recurring magnetic storms. Chapman and Bartels (1940) noted that this only occurred for moderate intensity storms, and that this feature is not present for the most intense events. We will verify this result and explain why the intensity dcpcndcncc exists.

The high speed stream/heliospheric current sheet (HCS) interactions will be examined by several case studies. The exceptionally high solar wind densities and the reversal of the field direction at the HCS allow several types of interactions to occur, interactions which can lead to southward IMF orientations and geomagnetic activity (Wilcox, et al., 1967).

DATA SELECTION AND METHOD OF ANALYSES

We have selected three years during the descending phase of solar cycle 20 for this study (1973-1975). This particular interval was chosen because of the presence of two long lasting coronal holes that provided high speed streams in the ecliptic plane (Hansen et al., 1976; Tsurutani et al., 1982; Lindblad and Lundstedt et al., 1983; Lindblad, 1990). Although all three years have been analyzed in detail, for purposes of illustration, wc will focus primarily on the year 1974 which is representative for all 3 years and also has the advantage of containing the cleanest, most unambiguous examples of recurring streams, We usc examples from this year to illustrate the main points of the paper.

In order to perform this study both low resolution (--1 hour) and high resolution (seconds to minutes) magnetic field and plasma data were needed. The former will be used to illustrate the large-scale timing features of the high speed streams and HCS events and the latter to study the detailed causes of the Bs events. We have used the OMNI IMP-8 1-hour averages of the interplanetary parameters for the former and have also obtained high resolution IMP-7 and -8 plasma and magnetic field data from the National Space Science Data Center, GSFC for the latter. Because the IMPs are Earth-orbiting spacecraft, there are interplanetary data gaps when the satellites enter the magnetosphere/magnetotail. These gaps unfortunately cannot be avoided.

Dst (1 hour), ap (3 hours) and AE (2.5 minutes) indices are used to study geomagnetic storms and substorms. These indices were obtained from the World Data Center A, Boulder, Colorado. Averaging of the AE index was performed where appropriate.

We usc the WDCA Ds_t indices unless stated otherwise. Some intervals such as the initial phases of storms can bc better studied with this pressure uncorrected Dst index, and thus the general usc of these values in this paper. It should be noted that for some other intervals, this can depart considerably from the solar wind-ram pressure corrected values. In Table 1, we show both the maximum uncorrected and pressure corrected Dst values.

RESULTS

I. Large Scale Structures

High Speed Stream and Magnetic Field Structures

Figures 1 and 2 illustrate hourly averages of the magnetic field and plasma data and geomagnetic indices for the year 1974. In Figure 1, from top to bottom, are the interplanetary magnetic field B_z component in GSM coordinates, Dst, solar wind velocity and the magnetic field magnitude. Figure 2, to the same scale, has B_x, B_y, solar wind ion density and temperature. Velocity is repeated in the middle panel of Figure 2 as a reference, so that this Figure can be related to features in Figure 1. At the top of both Figures, the IMF Sector crossings are indicated by vertical marks, with the + and - signs indicating positive and negative sectors. The sector crossings were taken from Svalgaard (1976). These values were derived from the Stanford solar magnetographs.

There are several important points to note in Figure 1. The first is that there are many high speed streams present (sometimes over two per solar rotation) with velocities up to 800 km s^{-1}. Most streams have characteristic profiles of a fast rise in velocity and a long decay (Schwenn, 1989; Marsh, 1991). Some excellent examples of this are the three streams from days 24-68 and the three streams from days 177-214. There are other streams which have profiles which indicate that the streams are composed of several superposed events. Examples can be found within days 161-176 (with "small" stream onsets on days 162, 163, 166 and 171) and within days 25-41 (with onsets on days 25, 28 and 30). Other streams are even more complex (see the interval between days 256-281).

However, examining the overall general features, one can clearly note that there are predominantly two main streams that occur during each solar rotation of ~ 27 days. This is most obvious for the consecutive 27-day periods of: days 24, 51, 78, 105, 132, 159, 186, 213 and 240. Stream onsets are present at each of those days. This sequence also extends back in time into 1973 and also forward into 1975, but with less apparent regularity as the events discussed above. For organizational purposes, we will refer to this recurring stream as the sequence 1 stream. A second sequence of streams, located in between the sequence 1 streams are found on days: 15, 41, 68, 95, 122, 150, 177, 204, and 231. We will refer to this second set of streams as sequence 2. Beyond day 231, the streams become somewhat more complex, so we will focus on the first 2/3 of the year.

The bottom panel of Figure 1 is the magnetic field magnitude. There are several features that one should note. First, the field strength is, in general, anticorrelated with the solar wind velocity. The magnetic field intensity is lowest (below average) when the spacecraft is within a high speed stream, particularly at and near the peak velocity and within the trailing portion of the stream. Examples from the ordered streams discussed earlier occur on days 27-34, 55-63, 70-74, 205-212, 217-226 and 233-23"1. Many other examples of this feature are present in this Figure. When the solar wind velocity is near a minimum value, -350 km S-l or less, the magnetic field can sometimes be slightly above average. This is particularly true if there is a high speed stream close by. However, cases where there are no nearby streams can be noted on days 8-11, 47-49, 131-136 and 198-203. The cause of this will be explored somewhat later. There are much higher field strengths coincident with low velocities that occur during the year, but the above cases were pointed out specifically because they occurred well away from the high speed stream interfaces. The high fields near the stream interfaces will be discussed below.

The highest field magnitudes that occurred during the year appear as spikes on these time scales. Most of these are located at the leading edges of the high velocity streams. Almost all of the large fields that have hourly averages greater than 15 nT are of this type. Examples are present on days 25-26, 150-151, 161-162, 176-177, 187, and 204. These events are not associated with interplanetary shocks (this will be illustrated later). The maximum peak (hourly average) intensities for these events mentioned above lie in the range of 15 to 25 nT. In the interval from day 1 to 240, where the streams are well-ordered and the data more-or-less complete, the fields at these stream interfaces are typically 10-20 nT. This somewhat lower number for the "average" case is due to the inclusion of weaker stream-stream interaction regions.

The maximum hourly average interplanetary magnetic field strength detected by the IMPs during this year was 30 nT. This is on day 187. This is the event listed as "A" and has been identified

as being associated with a CME (solar flare related) and is not associated with a corotating stream. This will be discussed in depth later.

Wc have also studied similar data for the years 1973 and 1975. From our analyses, we find essentially the same features in the magnetic field magnitudes. The lowest magnetic field strengths again occur within the high speed streams. Magnetic field spikes occur at the low velocity - high speed stream interfaces. In 1973, most of these field spikes had peak intensities of 15-30 nT, with only one event (day 104) having a field strength above 30 nT. In 1975, there was no event that had a field strength greater than 25 nT (however, there are a lot of data gaps). Part of this may be due to the declining stream velocities in the midpart of the year. This data will not be shown to conserve space.

Interplanetary Events Causing Magnetic Storms (D_{st})

The second pane] of Figure 1 is the hourly average D_{st} values for the year. There are two notable features in this data set. The first is there are only a few large magnetic storms during the entire year, only three storms with Dst intensives less than -100 nT. These are the previously mentioned event A, on day 187 (Dst = -205 nT), event B on day 257 (Dst = -140 nT), and event C (Dst = -115 nT) on day 285. Note that none of these three events are associated with the two corotating stream sequences discussed previously. All three of the high speed stream events are led by fast forward shocks. These streams do not reoccur at 27-day intervals (it is noted however, that the latter two events are separated by 28 days). We will later show that all three events are CME events. Event A will bc shown to be caused by three superposed streams. Event B is an impulse event which occurs where the corotating streams begin to become quite complex (as mentioned previously). Event C is duc to a very small stream whose peak velocity is less than 530 km s]. This latter event has a clean profile of a fast rise-slow decay signature and is impulsive in nature.

The next highest level of magnetic storm intensities during 1974 occurs in a narrow range of -85 nT $\leq$ Dst $\leq$ -70 nT. There are four storms in this grouping and they occur on days 75, 80, 108 and 204. Each of the events is associated with large, - 15 nT (hourly average) interplanetary magnetic field magnitudes. These large magnetic fields are located at high velocity/low velocity stream interfaces. None of the four events were led by forward shocks. The stream events on days 80 and 108 are sequence 1 corotating streams. The stream event on day 204 is a sequence 2 stream. The event on day 75 is a smaller (impulsive) stream located between the two main sequence corotating streams.

The storm intensities associated with the nicely periodic (27-day) sequence 1 and 2 stream structures are only modest at best. As noted above, from day 1 to day 241, during 9 solar rotations and 18 major corotating stream appearances, there were only 3 stream appearances associated with $D_{st} \leq -70$ nT values. Most (12 out of 18 events) of the above high speed streams cause only small D_{st} disturbances of $D_{st} \geq -50$ nT. Sometimes the geomagnetic disturbances were not even perceptible in the D_{st} index. Examples of this latter type of stream-storm relationship (small ≥ -25 nT disturbances , or no storm at all) arc present on days: 15, 41, 68, 95, 123, 134, 150, 162, 177, 231 and 241. The peak velocity, velocity gradient and peak magnet.ic fields of these streams are not much different from those that cause storms with greater intensity $D_{st} \leq -70$ nT. Other parameters must be important additional factors.

The top panel of Figure 1 is the IMF B_z component in GSM coordinates. Large southward magnetic fields are present (event B has a small data gap) during the three largest magnetic storms (A, B and C). Presumably, magnetic reconnection is the mechanism of solar wind energy input into the magnetosphere. Similarly, for the storms with - 85 nT $\leq$ Dst $\leq$ -70 nT caused by the corotating streams, there are large southward B_z spikes on days 74-75, 80, 108, and 204. Other large southward B_z spikes ($<$ -10 nT) can be noted on days 24-25, 75 and 214. These have corresponding moderate intensity storms.

Geoeffectiveness of the Two Corotating Stream Sequences

The two streams, sequences 1 and 2, vary in their geoeffectiveness from solar rotation to rotation, and over their stream lifetimes. Of the two sequences, the first is more geoeffective at the beginning of the interval studied. Sequence 1, starting on day 25, and progressing at 27 day intervals, caused peak Dst values of -65, -20, -75, -85, -45, -30, "A", -60 and -35 nT. The seventh event of the sequence near event A is indeterminate because the large "A" storm overshadows any activity associated with the corotating stream, From Figure 1, the reader can note that the velocity of the stream decreases steadily throughout the event. The peak velocity starts near - .800 km S-l and declines to - 600 km s^{-1} near the end of the sequence. The geoeffectiveness (D_{st} intensity) of the stream is not directly related to the stream velocity, however. All one can say is that D_{st} appears to be slightly more negative at the beginning of the sequence when the velocity was the highest.

Sequence 2, starting at day 15 (and progressing at 27 day intervals) caused peak Ds_t values of -20, -20, -310, -50, -30, -25, -40, -75, and -35 nT. The peak velocities of the streams at the beginning of the sequence have values of 600-650 km S-l. This value rises more or less continuously throughout the sequence until a peak velocity of 800-850 km S-l is reached for the

last four appearances of the stream. A sharp magnetic spike of magnitude 15-20 nT is present at the high speed stream-slow stream interfaces during the last appearances of this sequence. Again, there is not a direct relationship between peak solar wind velocity and Dst. All one can say is that Dst is slightly more negative at the end of the sequence.

Positive Dst Intervals

Two other features in the Dst plot are noteworthy. One is that there are several intervals where Dst has positive (- +10 to +20 nT) values for several days at a time. We believe that this is not an artifact of the zero-level setting of Dst. These features can be related to specific solar wind parameters. Examples of positive Dst events are found on days: 14, 40, 50, 78, 105, 132, and 227. The onsets of these events are gradual and the magnitude of Dst typically increases with time. The events start days before the appearance of the high speed streams. Each event is associated with a slow solar wind stream located between the two high velocity coronal hole streams. For the events mentioned above, the minimum solar wind velocity was approximately: 350, 3 IO, 330, 330, 310, 330, and 300 km S-l, respectively. The densities during these intervals are 20, 10, 7, 12, 10, 8 and 30 cm^{-3}, respectively. The densities are either typical of solar wind densities or slightly on the high side. Examining other intervals of similarly low solar wind speeds, one finds that Dst is positive or becomes more positive during these periods.

Dst Recovery

Another feature to note in the Dst panel of Figure 1 are the very long recovery phases for the small magnetic storms generated by the corotating high speed streams. Most recoveries last one week or even longer, or until the next stream arrives. This is substantially different than for storms that occur at and near solar maximum (a standard decay time of the solar maximum storms is < 10 hours, Gonzalez et al., 1989). In this Figure, long recovery phases are the rule rather than the exception. Some prime examples of this are found on days 25 to 35, 80 to 92, 108 to 122 for the sequence 1 streams and days 204 to 214 and 231 to 241 for the sequence 2 streams. Many other examples are present in the Figure and for those in 1973 and 1975 (not shown).

There are other, long-lasting low-level Ds, events that do not appear to have normal recovery phases. These events have Dst negative intensities that are relatively constant for days on end. Two good examples of this feature are present on days 52-60 and 135-138. Both of these events are associated with sequence 1 streams. On day 52 the Dst event onset coincides with a very small precursor solar wind stream prior to the main, high velocity stream and the Dst depression continues well into and beyond the high solar wind velocity peak.

The days 135-138 event is shown in higher temporal resolution in Figure 3. The panels are: the solar wind plasma parameters plus interplanetary magnetic field components and magnitude, and Ds_t. There is a small precursor stream on day 134 (Figure 1) prior to the sequence 1 stream. In Figure 3, the slow rise in velocity of the sequence 1 stream starts near the end of day 135 and continues throughout day 138. Dst lies between --10 nT and -50 nT for these four days. Thus, this region of more-or-less continuous 10 W- ICVC1 Dst occurs both on the trailing edge of the precursor stream and on the leading edge of the larger sequence 1 corotating stream.

The short-term decreases in Ds_t are clearly reflected in increases in AE. There is a more or less one-to-one correspondence between substorms (AE) and ring current increases (Dst decreases). Substorms are almost continuously occurring during this four-day interval, presumably causing the sporadic Dst decreases and preventing a full recovery of the ring current to quiet-day values. This continuous AE activity is a High Intensity Long Duration Continuous AE activity (HILDCAA) event. These substorms are caused by negative B_Z components which are parts of large amplitude Alfvén waves. Such a relationship between southward B_Z, AE increases and Ds_t decreases can be noted in the Figure.

All of the other long recovery phase events and those small storms without classical recoveries are associated with HILDCAA events. These in turn are associated with large amplitude Alfvén wave events where the wave components have significant negative B_z components. More on this topic will be stated in the following section.

Substorm (AE and ap) Relationship to Storms (D_{st})

Figure 4 gives the ap and AE indices for 1974 with the Dst index repeated as a reference. The AE and Dst indices have been averaged to 3-hour values to match those of ap. AE is exceptionally high for this year (283 nT). This has been previously noted by Saba (1992), In contrast, the 1979 AE average is only 221 nT, a year near solar maximum. However, it can be noted that AE rarely attains (hourly average) intensities above 1000 nT. All cases of high AE events occur during relatively large magnetic storms. The AE > 1000 nT intervals are found on days 75 (- 1000 nT), 94 (~ 1100 nT), 186-187 (~ 1100 nT), 204 (- 1000 nT), 241 (- 1000 nT), 259 (- 1050 nT), 286 (- 1000 nT), 289 (- 1100 nT), 291 (- 1000 nT), 293 (- 1100 nT), and 318 (- 1100 nT). Events on days 75,94, 186, 204, 286, 289 and 293 occurred during storm main phases. On days 187, 241, 259, 291 and 318, the peak AE events occurred during storm recovery phases. However, for the latter cases, it is usually possible to note significant ring

current intensifications (D_{st} decreases) associated with these AE events, indicating that intense substorms added significant amounts of fresh ring current energy into the magnetosphere.

We ask the question "if the peak AE values arc not exceptionally large, then what is it that causes the average AE value for 1974 to be unusually high?" This can be understood if we go back to the high speed stream sequences of Figure 1.

We compare the AE index to Ds_t for sequence 1. Starting on day 25, we note that AE reaches a peak intensity of - 730 nT within one-half day, corresponding quite closely (o the D_{st} decrease in the storm main phase. However, AE remains quite high for many days afterward, up through day 31 ancl beyond. Throughout this period, D_{st} generally recovers, but there are occasional small 10 to 20 nT decreases, indicating small ring current (energy) injections. The next occurrence of the high speed stream is on day 53. AE oscillates between -250 nT to ~ 750 nT from day 53 through day 60. The solar wind velocity declines from a peak value of ~ 750 km s^{-1} to -600 km s^{-1} throughout this interval. Dst has values between -10 and -20 nT with no indication of decaying further. Again, frequent small Dst decreases are associated with AE increases.

The next passage of this sequence 1 high speed stream occurs on days 79-80. A peak velocity of -750 km s^{-1} is reached on day 80 and the stream velocity decays to -540 km s^{-1} by day 86. On day 79 there is a sharp increase in AE to peak values between 500 to 750 nT. This occurs concurrently with the storm main phase. AE remains high until day 86 when there is a sharp but short drop and then a return to high values.

The other appearances of the stream are similar to those discussed above. We skip to the last event where the stream speed and strength has decreased substantially. The 8th appearance of the stream occurs on day 214. On this day, AE abruptly increases to -750 nT, decreases to 250 nT and increases again to - 800 nT on day 215. Two Dst decreases correspond to these two AE events. AE remains relatively high (100 to 500 nT) through day 222, after which AE decreases below 200 nT. The solar wind velocity decreases to < 500 km s^{-1} after day 222. The association between V_{sw}, AE and Dst is generally the same for stream sequence 2 and thus will not be discussed.

What are the interplanetary feature(s) causing this AE activity? Figure 5 gives an example of the IMF B_z component in substantially higher time resolution. Also included in the Figure are 2.5 minute AE averages, B magnitude and Ds_t. It can be noted from the B_z component of the field that the interplanetary magnetic field is highly turbulent. Some of these field fluctuations have

large southward values. A one-to-one correlation can be noted between the B_s and AE increases, indicating magnetic reconnection is driving magnetospheric substorms on Earth. Because the B_s events associated with these fluctuations are not as intense and do not last as long as those associated with the storm main phase events (here typically B_S - -5 to -10 nT with durations - 30 minutes to 2 hours), the ring particle current injections causing the Alfvén wave B_s events are not as substantial. Other periods have been examined with the same general findings.

A cross-correlation analysis of 24 hours of the plasma and magnetic field y-components is given in Figure 6. B_y and V_y are correlated at zero lag (0.65), indicating that these fluctuations are Alfvén waves propagating outward from the Sun. The southward deviations in the field associated with these waves are causing the high latitude (auroral) geomagnetic activity. Other 24 hour intervals where large amplitude B_z fluctuations were present were analyzed, We obtain similar correlation coefficients peaked at zero lag. If the time intervals of analysis are shortened to 12 or 6 hours, the c.c. coefficient can increase to 0.8 or larger.

These relatively intense AE events presented here are similar to the High-Intensity Long-Duration Continuous AE Activity (HILDCAA) events which were previously noted during solar maximum (Tsurutani and Gonzalez, 1987; Tsurutani et al., 1990). The only apparent difference is that the AE events discussed here do not necessarily stay above the 200 nT threshold for 48-hours with AE < 200 nT gaps less than 2-hours duration, the somewhat (arbitrary) HILDCAA definition. The important thing here is that physical mechanisms for HILDCAAS and this geomagnetic activity appear to be the same.

Thus, what appears to be the cause of the strong AE activity during 1974 is the presence of the two high-speed corotating streams that contain large amplitude Alfvén waves throughout the streams. The waves are almost continuously present, perhaps even more so than during solar maximum intervals. When this plasma impinges on the Earth's magnetosphere, the southward turnings associated with the wave fluctuations cause sporadic reconnection and the consequential sporadic (relatively) high level of AE activity. The waves appear to be most geoeffective when the solar wind velocities are near their maximum values. The AE amplitude is found to decrease with decreasing solar wind velocity, particularly when V_{SW} decreases below 500 km S-l. Velocity is probably not the physical cause, however. The wave amplitudes are larger in the region of peak velocity and decrease with decreasing velocity. The presence of two streams per rotation rather than one is an additional factor for creating the high annual AE average value.

Quiet AE Intervals

Intervals of low geomagnetic activity have been noted as well (see Figure 1). '1'here are small intervals where AE is less than 200 nT for days at a time. These events arc found to typically be associated with intervals that precede the onset of the high speed corotating streams. Examples of events somewhat prior to (but not exactly at) the sequence l streams are found on days 21-24, 49-50, 76-78, 102-106, 130-133, 156-158, and 224-230. Each of these intervals also partially overlap with intervals where Ds_t is positive. These positive D_{st} events were discussed previously,

Five of the seven low AE events mentioned above had common interplanetary features, 'In these cases, the velocities decreased from 560 to 310 km S-l, 520 to 300, 460 to 360, 530 to 360 and 400 to 360 (with a minimum of 3(IO km S-l), respectively. The magnetic field magnitudes ranged from 6 to 3 nT, 7 to 5, 6 to 8, 5 to 4, and 5 to 3 nT during these intervals, respectively. The 13_z component variability during these intervals was generally small. There is a general lack of the presence of Alfvén waves. There also may be a slight tendency for these intervals to have an average positive B_Z value. Examples of this are found on days 102-106, 130-133 and 156-158. This is most likely due to our criteria of the selection of the events. Other intervals which have slightly southward B_z components would also have slightly higher AE values, and these were probably overlooked as potential low AE events.

There are several plasma features that are generally consistent during the above five events. They occur on the trailing portion of high speed streams. The velocities start near 500 km s^{-1} and decrease with time. The temperatures also decrease and the plasma densities increase throughout the events. The densities start at values near the lowest detected in solar wind, -3 cm^{-3} and increase to substantial values as the HCS is approached. For the five cases, N increases from 23 to 65 cm^{-3} (just prior to the stream onset and HCS crossing at the start of day 25), 3 to 12 cm^{-3} (including a broad HCS crossing from days 105-106), 3 to 11 cm^{-3} (just prior to a HCS crossing at the end of day 133), 3 to 5 cm^{-3} (just prior to the HCS crossing on day 159) and 5 to 40 cm^{-3} (just prior to the HCS crossing at the beginning of day 231). The HCS crossing is identified by the vertical marks at the tops of Figures 1 and 2, separating the + and – sectors. These crossings can also be noted by the vertical 'marks at the tops of Figure l and 2, separating the + and – sectors. These crossings can also be noted by the sharp B_x and By polarity reversals. The higher ram pressures associated with the enhanced interplanetary densities and the lack of ring current energy injections (due to the lack of the presence of Bs) presumably are the causes of the positive D_{st} values.

The two events that did not follow this general pattern are found on days 49-50 and 76-78. The first occurred in a low solar wind velocity region, 340 to 430 km s^{-1}, just prior to the HCS crossing on day 51. The density was relatively high, 10 to 30 cm^{-3}. The magnetic field varied from 9 to 4 nT. Ail of these plasma and field features are similar to those occurring near the end of the previous 5 events. The only difference is that the event was not associated with a trailing portion of a high speed stream. The magnetic field was also distinctly northward during this interval.

The final quiet event of the seven, days 76-78, is associated with a small impulsive stream which is located midway between a sequence 2 stream (onset on day 68) and a sequence 1 stream (onset at the end of day 79). The small stream creates a large magnetic magnitude compression on days 75-76, and a magnetic storm onset on day 75 associated with an intense B_S event at the front end of the stream. In the quiet interval, the interplanetary magnetic field magnitude decreases from 15 nT to 5 nT and the density varies from 15 to 4 cm^{-3}. The HCS crossing occurs at the beginning of day 79, just after the quiet event. The main cause of this particular interval of geomagnetic quiet is the B_Z is positive throughout the stream interval.

27 Day Recurrence in ap Activity

The middle panel in Figure 3 is the ap index. This index is constructed from midlatitude magnetometer stations. The index is sensitive to and therefore represents both ring current and auroral activity. By using ap, one cannot tell if the activity is storm (Dst) activity or high latitude substorm (AE) activity. Ap is largest during the main phases of the largest storms: days 25, 75, 79-80, 108, 187, 204, 258, 286 and 315. However, the index also picks up both the sequence 1 and sequence 2 corotating stream Alfvén wave-related events as well. There is a clear 27-day periodicity in this index. The 1973 and 1975 data contains similar features. The , most intense ap intervals are those associated with impulsive streams (CME events), but, there are clear 27-day periodicities associated with the coronal hole-associated streams as well. Thus if one examined ap indices alone, one could obtain the impression that there were intense 27-day recurring geomagnetic storms rather than 27-day recurring intense high-latitude auroral activity (there are recurring magnetic storms but they are low in intensity). From these three years of study, there are no 27-day recurring intense ($D_{st} \leq$ -100 nT) magnetic storms (as defined by D_{st}).

D_{st} Power Spectra

The power spectra of 12 hour averages of Dst were made for the years 1973 and for 1974. These arc shown in Figure 7. Both years show a small peak at 28.9 days, roughly the solar rotation

period. There are also secondary peaks at approximately half [he rotation period, 12.9 days for 1973 and 14.5 days for 1974. These correspond to the temporal separation of the two streams. Presumably, there is a temporal (and spatial) shift from 1973 until 1974. In 1974 there is a third peak at 7.7 days. This may correspond to the CME events that arc interspersed between the two alternating streams. Whether this is a coincidental location or not (approximately one-quarter of the fundamental period of 28.9 days), is not known.

CASE STUDIES

Intense Storms During 1974

The above illustrations and discussion were presented to allow the reader to get a feel for the overall interplanetary causes of storms/substorms/geomagnetic quiet during the three years of the study. However, to obtain a more concrete picture of the B_S events causing the largest magnetic storms, we first examine the A, B and C storm events of 1974.

Event A

The "A" event storm was the largest during 1974. This was called out in the discussion of Figure 1. It can also be noticed in the Figure that the stream responsible for the storm does not reoccur either 27 days before or after. It is an impulsive event. In Figure 1 it can be noted that the storm is composed of 3 distinct main phase components, each main phase more intense than the previous one. These phases are related to three separate streams noted in the velocity panel. Each stream is impulsive rather than corotating.

In Figure 8, we show the high resolution B_Z, |B|, velocity, density and temperature values for the A event from 12 UT day 185 until 00 UT day 188. At 0109 UT day 185 there is a fast forward shock identified by abrupt |B|, V, and N increases (not shown). Although the first (quasiPerpendicular) shock crossing was rapid, the shock jump was relatively small due to the low stream velocity. The peak velocity was only 490 km S-l. The cause of the abrupt Dst decrease at the storm onset is shock compression of prior southward directed interplanetary magnetic fields. The field is -4.5 nT prior to the shock and decreases to -7.5 nT in the post shock region. This intensive B_S field lasts for over one hour. Beyond this time the field remains southward, but less intensely so for another 12 hours. At 1532 UT day 185, a second fast forward shock occurs (Figure 8). The peak stream velocity is again only ~ 490 km s-1. There is a sharp IMF discontinuity at 2245 UT day 185. The field changes from a northward value to one directed southward with a B_S component of - 9-12 nT. The field remains primarily southward

throughout this stream. The most intense main phase onset is related to a third, much larger stream. The velocity increases from an upstream value of - 450 km s^{-1} to a post-shock speed of 600" km s1. The magnetic field magnitude increases from 10 nT upstream to over - 25 nT downstream. The maximum fields occur from 0410 UT to -0500 UT, with a peak value of -35 nT. During this interval the field is primarily in the B_S direction. A peak Bs value of 32 nT was reached.

The field in the region from 0410 UT until 0640 UT was relatively smooth and devoid of larger amplitude waves and/or discontinuities. The plasma densities and temperatures are relatively high. The density is in the range of 20-40 cm^{-3} and (he temperature -2 x 10^5 K. The plasma data do not fit with the possibility of this being part of the driver gas (CME) for the event. The southward directed B_Z is most likely due to strong field directional distortions due to the stream-stream interactions.

Additional support for the argument that the intense B_S is due to the stream-stream interaction is provided by the detection of the heliospheric current sheet (HCS) in the interval 0315-0410 UT, in the shock/stream interface. The IMF changes from an inward (–) to an outward (+) polarity, across this broad, fluctuating boundary. The southward fields responsible for the third storm main phase must come from the stream on the + polarity side of the HCS.

Event B

This interplanetary event is another nonrecurring event led by an interplanetary shock (see Figure 1). The event is shown in high resolution in Figure 9. The storm sharp onset is caused by shock compression of preexisting southward fields. The B_z field is - -15 nT prior to the shock, becomes compressed to < -40 nT at the shock at 1350 UT day 258 and remains at high negative B_Z values until 1432 UT. B_Z then oscillates between +5 nT and -40 nT until 1622 UT where it remains at -40 nT. B_z maintains a -40 to -50 nT level until 1830 UT day 258.

What is the cause of the highly turbulent fields within the center of the above B_Z event? The answer can be found by looking at the other field components and the field magnitude. Prior to the shock passage, the IMF is in the orthospiral direction with large negative BY (- -10 nT) and an even larger negative B_z (- 15 to -20 nT) component. In the interval (1432 to 1622 UT) where B_Z varies from +5 nT to -40 nT, B_x is large and positive (20 to 30 nT) and By positive (O to 10 nT), but less intense than B_X. There are also large magnetic field magnitude decreases associated with the field directional changes, indicative of the presence of strong local currents. After the field fluctuation region, from 1622 UT and later, the B_X and BY fields are well ordered, with

values of -10 nT, +10 nT, respectively. This is the positive sector field orientation. Thus, one possible interpretation of the field fluctuations between 1432 and 1622 U-I' is that this is a multiple crossing of the heliospheric current sheet or the crossing of several separate current sheets. Prior [o the high-speed event, the plasma density is high and the velocity low (not shown) indicating an approach to this region. The clear orientation of the field afterward is perhaps the strongest evidence for the hypothesis of a current sheet crossing.

We have searched for a classical driver gas, but have not found any obvious regions. The fields between 1622 and 1830 nT and also between 1955 and 2220 UT are large and somewhat devoid of waves, particularly the latter. Only the latter interval has low plasma densities ($< 1\ cm^{-3}$). However, the temperature remains high (- 6-8 x 10^5 K) throughout this region.

Event C

The third most intense storm during 1974 is again associated with a nonrecurring high speed stream led by a fast forward shock (Figure 10). The shock event occurs at 1245 UT day 285 where the magnetic field magnitude increases from 5 nT to - 12 nT, the velocity from 400 to 500 km s-l, and density from 7 to $30+cm^{-3}$. Shock compression of the interplanetary fields increases B_Z from +5 nT to +12 nT. The initial phase of the storm starts with the shock passage,

The southward IMF responsible for the storm is associated with the driver gas (CME). This is clearly denoted by the smooth magnetic fields detected at 2100 UT extending to 0135 UT day 287 (terminated by the spacecraft entrance into the Earth's magnetosheath). The fields are large and smooth with little wave intensity and essentially no discontinuities. The plasma temperature is low -4 x 10^4 K throughout this region. This is consistent with the standard picture of a driver gas (Zwickl et al., 1983; Tsurutani et al., 1988). The magnetic field B_z decreases to -15 nT and remains at about this large value until 1000 nT day 286. Near the end of the driver gas at 0130 UT day 287, the B_Z component rises to +5 nT.

Solar Sources

Possible solar sources for the three high speed streams (A, B, C events) are given in Table 1. These solar events were obtained by examining the Solar Geophysical Data (Boulder, CO) and the World Data Center A for Solar-Terrestrial Physics, Report UAG-52. The velocity of the high speed stream at 1 AU was also used to rule out events that would require unreasonably high or unreasonably low transit speeds.

Event A. Three small 1B/2B flares were the most intense events during this period. Because event A is a compound event involving 3 interplanetary shocks, onc might hope that these three flares would correspond to the three interplanetary shocks at 1 AU. However, (hc timing for the first two flares were within 24 hours of the detection of the shocks at 1 AU. Such unreasonably short transit times rule out these flares as possible sources.

The solar flare event at 02S9 UT day 184 is the only event that fits any of the three shocks time-wise. If one considers the last shock occurring at -00 UT day 187, an average speed of -604 km s^{-1} is determined. This is in good agreement with the measured post shock flow velocity of - 600 km s^{-1}.

Event B. The interplanetary shock is detected at 1350 UT day 258. The post shock flow speed is -645 km s-1. Assuming a constant flow from the Sun to the Earth, this would correspond to a transit time of -2.7 days. The 2B flare on 13 September is the only reasonable candidate. There were no prominence disappearance events during the interval of interest.

If this solar event is the cause of the high speed stream, the stream would have to have had an average transit speed of -850 km S-l. This is somewhat high considering the measured speed at 1 AU. Significant deceleration is possible however. The flare on 10 September would lead to an average transit speed of 370 km s^{-1}. This event can therefore be ruled out.

Event C. The shock was detected at 1 AU at 1245 UT day 285. The only prominent flare occurred on day 284 at 0325 UT. There were no prominence disappearance events in the time interval of interest. The 2B flare occurred less than a day and a half prior to the detection of the shock at 1 AU. Because the stream velocity was quite low - 500 km s^{-1}, this solar event seems unlikely of being related to the storm-causing stream.

It is interesting to note that it has been difficult to identify the solar events that are associated with the storm-causing streams at 1 AU. The solar sources for two of the three major events, B and C, are uncertain at best. It is possible that none of our identifications are correct. These impulsive events may not have had optical counterparts.

HCS Crossings and Geomagnetic Activity

We have examined all of the other magnetic storm events occurring during 1974 with $D_{st} \leq -50$ nT. We wish to determine if there is a dependence on the IMF polarity, a dependence that might be present if the equinoctial hypothesis is the predominant cause of these smaller storms (Russell

and McPherron, 1973; Crooker et al., 1992). We have also looked to see if there is a storm seasonal dependence. There arc 14 $D_{st} \leq$ -50 nT events in all. Seven of these are associated with HCS +/- crossings and seven arc associated with -/+ crossings. Thus, there is no obvious HCS polarity dependence. We should point out that although there is no HCS crossing dependence, there is some evidence that negative sectors within March-April and positive sectors with Scptcn~bcr-October tend to favor Dst enhancement, in agreement with the Russell-McPhcrron mechanism. This can be found in Figure 1. We should point out that although there is no HCS crossing dependence, there is some evidence that negative sectors within March-April and positive sectors within September-October tend to favor D_{st} enhancement, in agreement with the Russell-McPherron mechanism. This effect can be seen in Figure 1.

Wc have also briefly examined the Dst and IMP-8 data to determine if there is a seasonal dependence of magnetic storms. We find no clear indication of a seasonal variability in the storms of 1 '974, as seen in the Dst panel of Figure 1, converse to the strong features observed for intense Dst $\leq$ -100 nT storms (Gonzalez and Tsurutani, 1991; 1993).

Corotating Streams and their Relationship to HCS Crossings

To illustrate the types of phenomena that are associated with southward B_z's that lead to the moderate Dst magnetic storms during 1974, wc show two specific interplanetary corotating storm examples. We will examine our high speed corotating stream events at the beginning of the sequence 1 streams, and an event near the end of the sequence 2 streams.

Day 25

Prior to the beginning of the event illustrated (Figure 11), the field has exceptionally low values of - 1 nT at 1445- 1700 UT day 24 and has an orientation that is neither in a + or – sector polarity (see Figures 1 and 2). The solar wind has an exceptionally low velocity (300-310 km s^{-1}) as well as a low temperature (- 2 x 10^4 K). The plasma density was high, -20-30 cm^{-3}. These plasma features give a good indication that the spacecraft (and Earth) is probably near the HCS. The low magnetic field strengths (and therefore low potential B_z values) cause very low AE values.

With increasing time from 1700 UT day 24 to 1200 UT day 25, there are steady trends in several of the plasma parameters. The magnetic field increases from -- 1 nT to 25 nT. N increases from 15 cm^{-3} to 80 cm^{-3} (at ~ 0500 UT) and then decreases to 30 cm^{-3}. There are no significant velocity and temperature gradients until -0400 UT day 25. At this time the velocity starts at 330

km s-1 and rises, and the temperature starts at 3 x 10^4 K and rises . By 1200 UT, day 25, V_{SW} ~ 450 km s-1 and T -5.5 x 10^5 K. The increasing plasma density leads to an increase in the solar wind ram pressure and hence a peak Dst of - + 35 nT at -02 UT day 25.

Beyond 1200 UT day 25, the velocity continues to increase, reaching a maximum of 775 km s^{-1} at -0030 UT day 26. The temperature reaches a maximum of -6 x 10^5 K from 1300 to 1910 UT day 25 and suddenly decreases to 4 x 10^5 K at 1910 UT. This decrease is due to the presence of a reverse shock. The solar wind velocity jumps from 620 km s^{-1} to 740 km s^{-1}, the density abruptly decreases from 12 to 5 cm^{-3} and the magnetic field magnitude decreases from 22 to 10 nT. This example of a reverse shock occurring at 1 AU without the presence of a forward shock is fairly common in the data studied. one speculation for the lack of a companion forward shock is the presence of unusual plasma conditions near the HCS and its plasma sheet. Although the density is very high (up to 80 cm^{-3}) at this interaction region, the intense magnetic field strength |B| -25 nT developed from the stream-stream interaction is unusual] y large as well. After 1300 UT day 25 where the velocity gradient is steepest. the density is 30 cm^{-3} and decreasing. The field is a relatively constant -25 nT. Thus the local Alfvén speed is 70 km s^{-1} at 1300 UT and increases with time. The solar wind speed is only 480 km s^{-1}, so the lack of a stronger velocity gradient and the relatively high Alfvén wave speed may prevent a forward shock from forming.

The location of the HCS is somewhat difficult to place in this case. The IMF is clearly on a negative sector polarity (positive B_x, negative By) after -00 UT day 25. Prior to that time the polarity is mixed or is in an orthospiral direction. Thus, if we follow this interpretation of at least one crossing of the HCS, the largest densities are on the same side of the HCS as the high speed stream.

The B_Z that causes the storm is clearly related to the stream interaction with the HCS and its plasma sheet. B_Z steadily decreases from + 3 nT at 1200 UT day 24, to -10 nT at 0400 UT day 25 as the HCS plasma sheet density increases from 12 to 60 cm^{-3}. The most intense southward B_Z field during the event occurs from 0600 UT to 0655 UT day 25 with a peak intensity of -16 nT. This intense southward IMF is coincident with the magnetic storm onset. The location of this B_Z event is found at the base of the HCS plasma sheet/stream interface. The velocity of the stream is only 370 km s^{-1} at the time. It should be noted that pressure corrections have not been removed from D_{ST}. Thus, the Dst values may be significantly lower than indicated, particularly from 2-18 lJT day 25.

Day 177

The corotating stream event is illustrated in Figure 12. At 1200 UT day 176, well prior to the stream onset, V_{SW} -- 315 km s-], N ~10 cm^{-3}, T ~ 5 x 10^4 K and |B| - 6 nT. At the very beginning of the stream gradient, -00-06 UT day 177, the density increases to 35-65 cm^{-3}. The increased solar wind ram pressure causes D_{st} m reach - + 35 nT during this interval. Since the solar wind velocity increase is only slight, the D_{st} increase is duc almost entirely to the density enhancement.

The magnetic field magnitude also abruptly increases with the density increase. Peak values of - 25 nT are reached near - 06 UT day 177. However, somewhat different than the plasma density profile, the magnetic field intensity remains high until ~ 15 UT day 177. Thus the density enhancement is located at the very base of the corotating stream and the magnetic field enhancement within the stream gradient. The corotating stream peak intensity of 750-800 km s^{-1} is attained at -00 UT day 178 when the field has decreased to a steady -7 nT.

The location of the HCS can be noted by examining the IMF BY and B_x components. Prior to ~ 05-06 UT day 177, BY is generally negative and after that time BY is positive. There is a broad discontinuity from ~ 05 to 06 UT where BY reverses sign. Prior to -05 UT, B_x is positive and after - 10 UT B_x is generally negative. Thus one can possibly interpret the -05 to 06 UT interval as a crossing from a negative sector field to a positive sector field.

The largest and longest duration negative B_z event occurs at this transition. B_z has a value of -- 15 nT for -1 hour. This is related to the BY sign reversal. The negative B_z event marks the start of the small storm ($Ds_t \leq$ -15 nT). If pressure corrections are taken out (they have not been removed from this part of the study), the D_{st} values could be much more negative. Subsequent negative B_z values on days 178-179, associated with Alfvén waves lead to a peak Ds_t --45 nT on day 178.

DISCUSSION AND CONCLUSIONS

Three years of interplanetary and geomagnetic data (1973-1975) have been examined to determine [he solar wind features that are responsible for geomagnetic storms (D_{st}) and auroral zone substorms (AE) during the descending phase of the solar cycle. In 1974, it is found that only three storms with intensity $Ds_t < -100$ nT occurred, All three of these events were caused by high speed streams led by forward shocks. In one event, a clearly identifiable magnetic cloud

was detected. Solar flares were possibly associated with some of the events. Thus, during 1974, we argue that all major $Dst \leq -100$ nT storms were associated with CMEs.

The specific mechanisms creating southward IMFs causing two of the magnetic storms was shock compression of preexisting southward fields plus compression of embedded HCSs. In the third case the southward fields were associated with a magnetic cloud within a driver gas.

The most noticeable interplanetary feature during 1974 is the high speed corotating stream structures (Figures 1 and 2). There are two almost equally spaced streams, each of which recur every 27-28 days at Earth. These streams can generate moderate (-100 nT $\leq Dst \leq -50$ nT) to weak x($-50 \leq$ Dst ≤ -25 nT) recurring magnetic storms at Earth. It must be noted, however, that the corotating streams sometimes have little or no effect at all ($O \geq$ Dst > -25 nT).

The largest magnetic field magnitudes associated with the corotating streams occur at the leading antisolar edges where the stream runs into the upstream high density heliospheric current sheet (and its plasma sheet). Part of this field is due to the interaction and partisan intrinsic feature of the HCS itself. The peak hourly average fields lie in the range of 15 to 25 nT. These field strengths are less than those typically associated with either the sheath or driver gas of an impulsive solar event (CME) detected at 1 AU. The direction of the IMF within this high-field portion of the corotating stream is often highly fluctuating. Long duration intense southward fields ($B_z < -10$ nT, T > 3 hours) are typically not present. These are the reasons for the lack of intense (Dst ≤ -100 nT) magnetic storms associated with recurring streams.

Figure 13 illustrates the corotating stream interaction with the heliospheric current sheet. At the top of panel a) is the quiet solar wind. The view is down from over the north ecliptic pole. At the bottom of the panel, the straight arrows represent the high speed corotating stream. The interaction of this stream with the HCS leads to compression of the fields and plasma, enhancing both the plasma densities and the magnetic field magnitudes. Because of the curvature of the magnetic fields, this stream-stream interaction is only a glancing one and yields a slow compression, like a slow snow-plow effect. There is some heating taking place, but not nearly the amount that would occur at a shock.

The bottom panel, b), shows a side view from the ecliptic plane. Here we have drawn the HCS with a substantial north-south orientation. The fast-stream interaction will distort the shape of the HCS and fields draped around this structure. Random north-south B_z components will be created from this interaction, leading to small storms.

In contrast m the storm activity, in 1974 the substorm (AE) activity was unusually high. The 2.5 min. AE average (1974) was 283 nT in comparison to 221 nT in 1979. 1979 was characterized hy many large magnetic storms. We find the cause for the high 1974 AE value is HILDCAA - like activity (continuous auroral activity) lasting for up to 10 days or more. The substorms are caused by the southward components of the Alfvén waves contained within the high speed corotating streams. Since the two streams, sequences 1 and 2, take up a great portion of the 27 day solar rotation period, the variable fields are almost always impinging upon the magnetosphere. The continuous presence of these two streams and Alfvén waves throughout 19'74 is the reason for the unusually high aurora] activity.

Quiet intervals were also noted. Large intervals of positive Dst and intervals where AE was less than 200 nT for days at a time were found. These two types of intervals overlapped sometimes, but not always. They are both related to the passage of the heliospheric current sheet and its plasma sheet, but to different parts. Quiet AE intervals occur during the descending portion of high speed streams where the magnetic field is exceptionally weak. There is usually an absence of Alfvén fluctuations on this tail end of the streams as well. The plasma density increases slightly during these intervals, as the HCS is approached. Positive Dst occurs during low solar wind velocities ($V_{SW} < 350$ km s^{-1}) where the density is very high, i.e., within the HCS plasma sheet proper. The unusually high densities give a relatively high solar wind ram pressure. The compression of the magnetosphere causes the positive Dst values.

A schematic of geomagnetic active intervals and geomagnetic quiet is given in Figure 14. Region (1) is the distant trailing portion of a high speed stream. The velocity is relatively low and it is decreasing with time. The magnetic field magnitude is low and devoid of Alfvén waves. This is a region where AE is lowest (other than times when B_Z is northward for long intervals of time). In region (2), the plasma density is high due to the presence of naturally occurring high densities near the HCS and also due to stream-stream compressive effects. This region, when incident on the magnetosphere, leads to positive Dst values. If the IMF has significant southward components after the passage of this density enhancement, then this positive Dst will appear as an initial phase of the storm (without a sudden commencement). If there are not trailing southwardly directed fields, this will only be a positive Dst event. Region (3) has the high magnetic fields associated with the HCS and the stream-stream compressive effects. Distortions of the HCS and related high fields cause north and south deflections and the latter lead to small or moderate magnetic storms. Note that at 1 'AU this high field region is located at the beginning of the gradient of the high speed stream, and is not near the region where the gradient or velocity are the highest. Region (4), at the peak and trailing portions of the high speed stream, is

characterized by Alfvénic fluctuations in B_z and concomitant continuous auroral activity (HILDCAAs).

We find a ~ 27 day recurrence in ap activity. Most of this response is associated with recurring geomagnetic substorms and not magnetic storms. As mentioned previously, there are recurring magnetic storms, but these are relatively weak in D_{st} intensity (- 100 nT $\leq D_{st}$).

Why does the idea of 27 day recurring magnetic storms persist? At the time of the Chapman and Bartel (1940) book, only midlatitude indices such as ap were available. From these indices, onc could not tell if the geomagnetic activity was due to storms or substorms. From this study we clearly show both are present. However, we note that the dominant cause of ap periodicity is the long duration auroral activity (HILDCAAs) throughout the corotating stream.

Acknowledgments. Portions of this work were done at the Jet Propulsion Laboratory, California Institute of Technology, under contract with the National Aeronautics and Space Administration. We wish to thank E. J. Smith and J. Feynman for helpful scientific discussions.

REFERENCES

Burlaga, L. F., K. W. Behannon, and L. W. Klein, Compound streams, magnetic clouds, and major geomagnetic storms, J. Geophys. Res., 92, 5725, 1987.

Campbell, W. H., Occurrence of AE and Dst geomagnetic index levels and the selection of the quietest days in a year, J. Geophys. Res. 84, 875, 1979,

Chapman, S. and J. Bartels, Geomagnetism, 1, Chapter XII, 396, Clarendon Press, Oxford, England, 1940.

Crooker, N. U., E. W. Cliver and B. T. Tsurutani, The semiannual variation of great geomagnetic storms and the postshock Russell-McPherron effect preceding coronal mass ejects, Geophys. Res. Lett., 19, 429, 1992.

Feldman, W. C., S. J. Schwartz, S. J. Bame, D. N. Baker, J. Biro, J. T. Gosling, E. W. Hones, Jr., D. J. McComas, J. A. Slavin, E. J. Smith and R. D. Zwickl., Evidence for slow-mode shocks in the deep geomagnetic tail, Geophys. Res. Lett., 11, 599, 1984.

Feynman, J. and X. Y. Gu, Prediction of geomagnetic activity on time scales of one to ten years, Rev. Geophys., 24, 650, 1986.

Gonzalez, W. D. and B. T. Tsurutani, Criteria of interplanetary parameters causing intense magnetic storms (Dst < - 100 nT), Planet. Space Sci. 35, 1101, 1987.

Gonzalez, W. D., B. T. Tsurutani, A.L.C. Gonzalez, E. J. Smith, F. Tang and S. 1. Akasofu, Solar wind-magnetosphere coupling during intense magnetic storms (1978- 1979), J. Geophys. Res., 94, 8835, 1989.

Gonzalez, W. D. and B. T. Tsurutani, Terrestrial response to eruptive solar flares: geomagnetic storms, in Eruptive Solar Flares, ed. by Z. Svestka, B. V. Jackson and M. E. Machado, Springer, Verlag, 277, 1992.

Gonzalez, W. D. and B. T. Tsurutani, Interplanetary -magnetosphere coupling from ISEE-3, to appear in Proc. Sol. Terr. Energy Prog. (STEP) Symp., 1993.

Gonzalez, W. D., A. L. C. Gonzalez and B. T. Tsurutani, Comment on "The semiannual variation of great geomagnetic storms and the postshock Russell-McPherron effect preceding coronal mass ejecta", Geophys. Res. Lett. 20, 1659, 1993.

Gosling, J. T., D. J. McComas, J. L. Phillips and S. J. Bame, Geomagnetic activity associated with Earth passage of interplanetary shock disturbances and coronal mass ejections, J. Geophys. Res., 96, 7831, 1991.

Hansen, R. T., S. F. Hansen and C. Sawyer, Long-lived coronal structures and recurrent geomagnetic patterns in 1974, Planet. Space Sci., 24, 381, 1976.

Harrison, R. A., Solar coronal mass ejections and flares, Astron. Astrophys. 1.62,283, 1986.

Harrison, R, A., Coronal transients and their relation to solar flares, Adv. Space Res., 11, 25, 1991.

Hoeksema, J. T. and X. Zhao, Prediction of magnetic orientation in driver gas associated - B_Z events, J. Geophys. Res., 97, 3151, 1992.

Hundhausen, A. J., Sixes and locations of coronal mass ejections: SMM observations from 1980 and 1984-1.989, J. Geophys. Res., 98, 13177, 1993.

Klein, L. W. and L. F. Burlaga, Interplanetary magnetic clouds at 1 AU, J. Geophys. Res., 87, 613, 1982.

Lindblad, B. A. and H. Lundstedt, A catalogue of high-speed plasma streams in the solar wind 1975-1978, Solar Phys., 88, 377, 1983.

Lindblad, B. A., Coronal sources of high-speed plasma streams in the solar wind during the declining phase of solar cycle 20, Astrophys. Space Sci., 170, 55, 1990.

Low, B. C. and D. F. Smith, The free energies of partially open coronal magnetic fields, & J., 410, 412, 1993.

Marsch, E., Kinetic physics of the solar wind plasma, in Physics of the Inner Heliosphere II, ed. R. Schwenn and E. Marsch, 45, Springer-Verlag, 1991.

Russell, C. T. and R. L. McPherron, Semiannual variation of geomagnetic activity, J. Geophys. Res., 78, 92, 1973.

Saba, M. M., Intercomparison of the AE, ap and Dst indices for years near solar maximum (1979) and solar minimum (1974), M.S.c. thesis, Nat. Inst. Space Res., Sao Jose dos Campos, SP, Brazil, 1992.

Schwenn, R., Transport of energy and mass to the outer boundary of the Earth system, 13, 1989.

Smith, E. J. and J. H. Wolfe, Observations of interaction regions and corotating shocks between one and five AU: Pioneers 10 and 11, Geophys. Res. Lett., 3, 137, 1976.

Smith, E. J., J. A. Slavin, B. T. Tsurutani, W. C. Feldman and S. J. Bame, Slow mode shocks in the Earth's magnetotail: ISEE-3, Geophys. Res. Lett., 11, 1054, 1984.

Svalgaard, L., Interplanetary sector structure 1947-1975, Report 648, Inst. Plasma Res., Stanford Univ., Stanford , California, 1976.

Tang, F., B. T. Tsurutani, W. D. Gonzalez, S. I. Akasofu and E. J. Smith, Solar sources of interplanetary southward B_z events responsible for major magnetic storms (1978- 1979), J. Geophys. Res., 94, 3535, 1989.

Timothy, A. F., A. S. Krieger and G. S. Vaiana, The structure and evolution of coronal holes, Sol. Phys., 42, 135, 1975.

Tsurutani, B. T., E. J. Smith, K. R. Pyle and J. A. Simpson, Energetic protons accelerated at corotating shocks: Pioneer 10 and 11 observations from 1 to 6 AU, J. Geophys. Res., 87, 7389, 1982,

Tsurutani, B. T. and W. D. Gonzalez, The cause of high intensity long-duration continuous AE activity (HILDCAAs): Interplanetary Alfvén wave trains, Planet. Space Sci., 35, 405, 1987.

Tsurutani, B. T., W. D. Gonzalez, F. Tang, S. I. Akasofu, and E. J. Smith, Origin of interplanetary southward magnetic fields responsible for major magnetic storms near solar maximum (1978-1979), J. Geophys. Res., 93, 8519, 1988.

Tsurutani, B. T., T. Gould, B. E. Goldstein, W. D. Gonzalez and M. Sugiura, Interplanetary Alfvén waves and auroral (substorm) activity: IMP-8, J. Geoph~.w,%,2241, 1990.

Tsurutani, B. T., W. D. Gonzalez, F. Tang and Y. T. Lee, Great magnetic storms, Geophys. Res. Lett., 19, 73,.1992.

Wilcox, J. M., K. H., Schatten and N. F. Ness, Influence of interplanetary magnetic field and plasma on geomagnetic activity during quiet-sun conditions, J. Geophys. Res., 72, 19, 1967.

Wolfson, R., C. Conover and R. M. E. Illing, The evolution of a coronal streamer prior to mass ejection, J. Geophys. Res., 92, 13641, 1987.

Zirker, J. B., Coronal Holes and High Speed Wind Streams, Col. Asso. Univ. Press, Boulder, co., 1977.

Zwickl, R, D., J. R. Asbridge, S. J. Bame, W. C. Feldman, J. T. Gosling, and E. J. Smith, Plasma properties of driver gas following interplanetary shocks observed by ISEE-3, Solar Wind Five. NASA Conf. Publ., cP-2280, 711, 1983.

FIGURE CAPTIONS

Figure 1. The IMF B_Z, D_{st}, V_{SW} and IMF|B| for 1974. The three largest intensity magnetic storms are called out as the A, B and C events. The.sc storms arc caused by impulsive solar when events (CMEs) and are not related to corotating streams. The sectors are denoted at the top of the figure.

Figure 2. Same format as Figure 1, but for IMF B_X, By, Vsw, N and T.

Figure 3. D_{st} in a "recovery" phase of a magnetic storm. V_{SW}, N, T, the IMF, AE and D_{st} for days 135 to 138, 1974. The ring current does not have a classic decay profile, but is within the range of -- 10 to -50 nT for days. D_{st} decreases are accompanied by southward B_Z events and AE increases. Presumably, magnetic reconnection through the B_Z southward turnings cause the injections of fresh plasma into the magnetosphere, leading to slight pumping ups of the ring current.

Figure 4. Hourly average, ap, AE and D_{st} for 1974.

Figure 5. B magnitude, B_z, AE and D_{st} for day 136, 1974. The relationship between B_S increases and AE increases and slightly delayed D_{st}, is apparent.

Figure 6. Cross relation between V_y and BY for day 136, 1974. The peak correlation coefficient at zero lag indicates that the By and V_y fluctuations are Alfvén waves propagating outward from the Sun.

Figure 7. Power spectra of 12 hour averages of Dst for 1973 (left panel) and for 1974 (right panel).

Figure 8. Two of the streams and shocks responsible for the day 185-187 magnetic storm (the A event). The solar wind velocity, density, magnetic field magnitude and B_Z component arc displayed. Hourly average Dst is given in the bottom panel.

Figure 9. The B storm event. The Bs event responsible for the storm is created by shock compression of upstream B_S fields.

Figure 10. The C storm event. The storm is created by Bs within the driver gas.

Figure 11. The Dst - - 65 nT storm created by a corotating stream/heliospheric current sheet (HCS) interaction on day 25, 1974.

Figure 12. A D_{st} - -45 nT magnetic storm created by a corotating stream/HCS interaction on days 177-1'18.

Figure 15. Schematics of the corotating stream-HCS interaction: panel a) view from the north ecliptic pole, and b) view from the ecliptic plane.

Figure 14. A schematic of the solar wind causes of geomagnetic quiet, HILDCAAs and small magnetic storms during the descending phase of the solar cycle.

TABLE CAPTIONS

Table 1. Possible solar sources of the interplanetary (forward shock-led) high speed streams causing the A, B and C magnetic storms.

Table 1

A. Day 1815-187 (JULY 4-6, 1974)

•7/3	0259-0318-0412	1B	S15E9	Region 13043	
•7/4	0801-0840-0928	2B	S14E8	Region 13043	Type IV
•7/4	1338-1357-1442	2B	S16W8	Region 13043	Type 11/IV Intense microwave bursts

• Prominence Disappearance: Between 7/2 and 7/3 S15W20

POSSIBLE SOURCE: Flare on7/3at0259 UT.

B . Day 258 (September 15, 1974)

•9/10	2121-2150-2300	2B	N1OE60	Region 13225	Type 11/IV
•9/13	1510-1528-1802	2 B	S9E24	Region 13224	Type II/IV

• Prominence Disappearance: None between 9/9 and 9/15

POSSIBLE SOURCE: Flare on 9/13 at 1510 UT?

C. Day 258-286 (October 12-13, 1974)

•10/11	032.5-0331-0402	2B	N12E2	Region 13280	Type 11/IV

• Prominence Disappearance: None between 10/6 and 10/12

POSSIBLE SOURCE: Flare on 10/11 at 0325 UT?

SOLAR WIND – MAGNETIC STORM CORRELATIONS

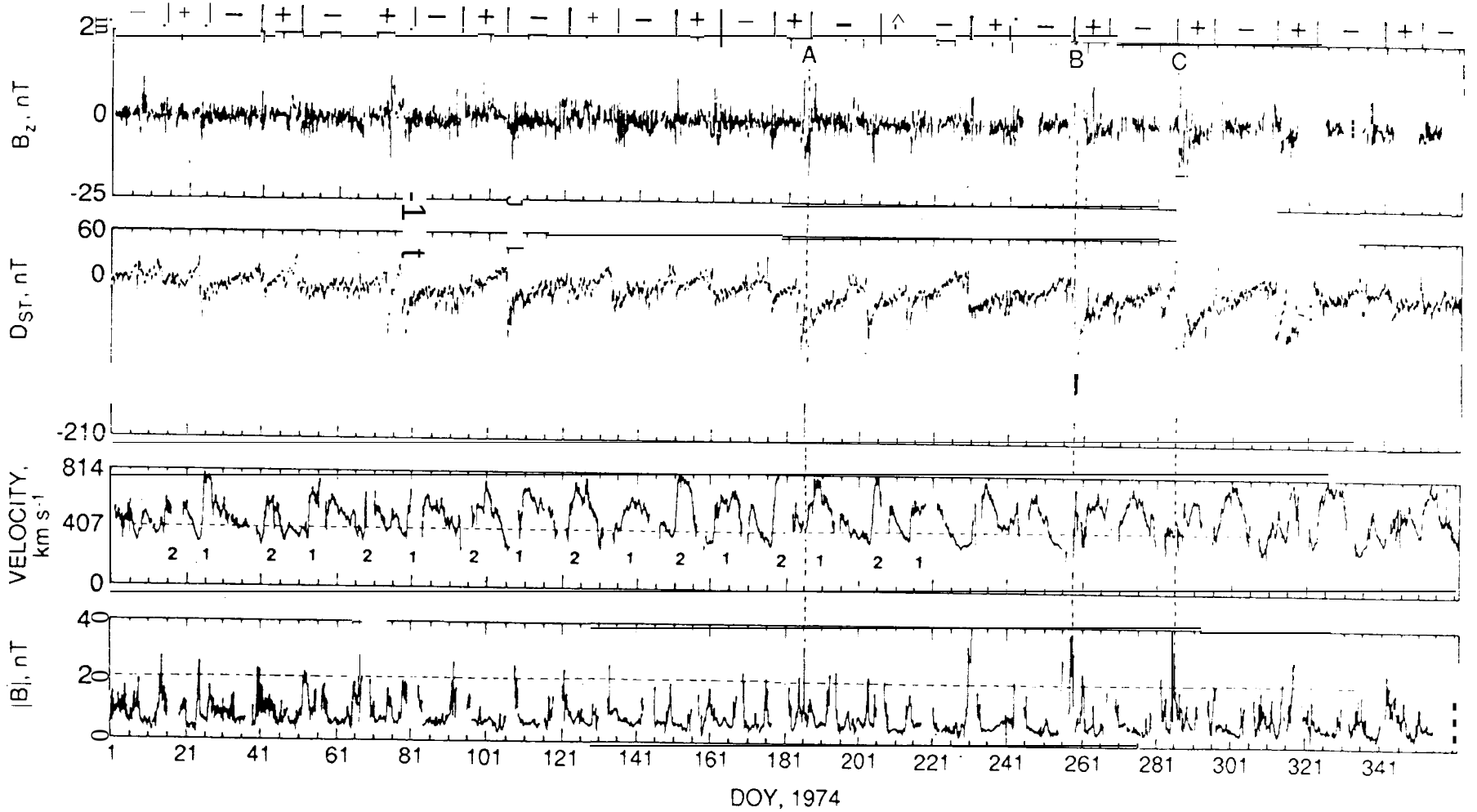

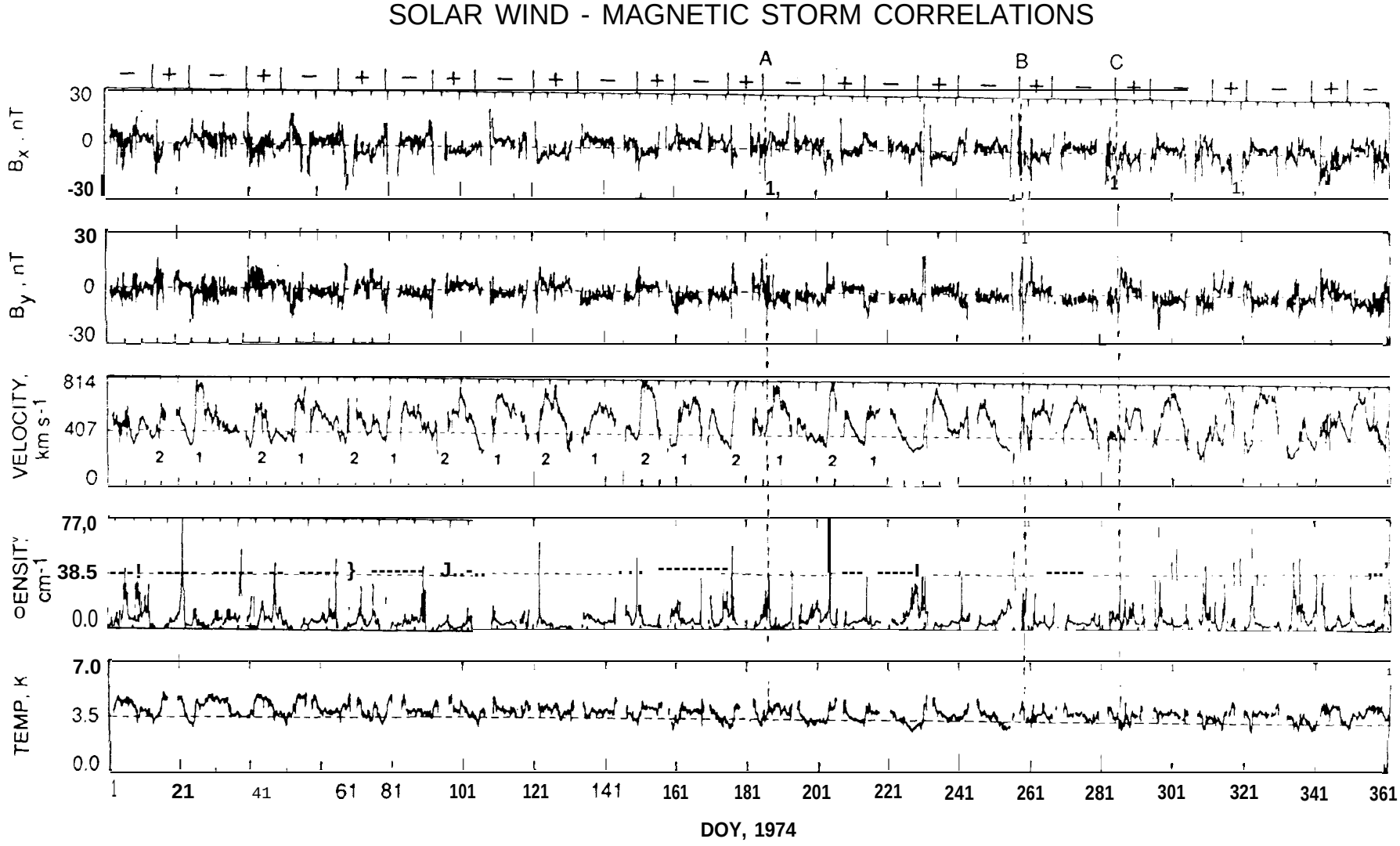
SOLAR WIND - MAGNETIC STORM CORRELATIONS
A
B
C
30
0
-30
B_x, nT
30
0
-30
B_y, nT
814
407
0
VELOCITY, km s^{-1}
77,0
38.5
0.0
DENSITY, cm^{-3}
7.0
3.5
0.0
TEMP, K
1
21
41
61
81
101
121
141
161
181
201
221
241
261
281
301
321
341
361
DOY, 1974

Figure 2

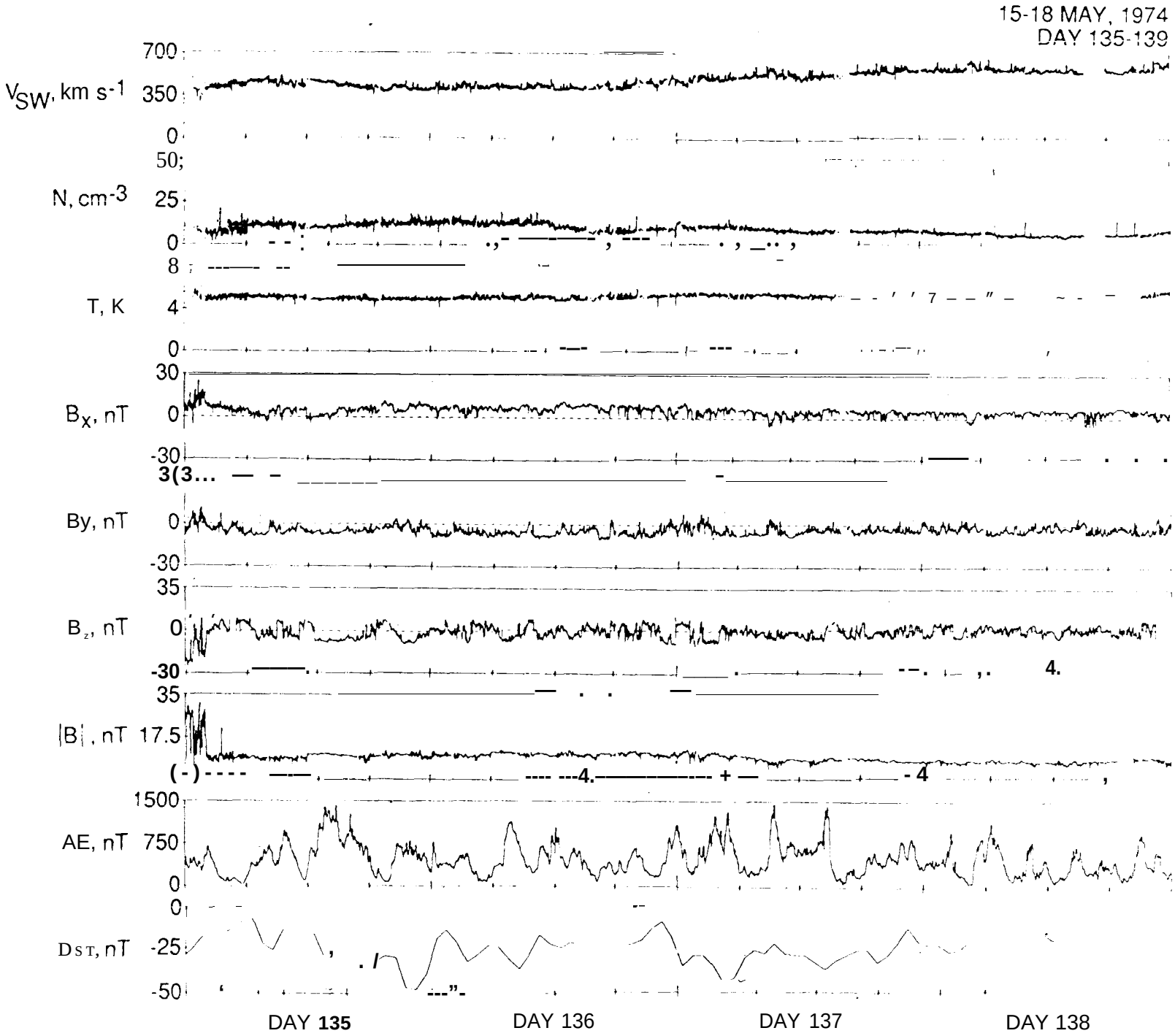
15-18 MAY, 1974
DAY 135-139
700
V_{SW}, km s-1
350
0
50;
N, cm-3
25
0
8
T, K
4
0
30
B_X, nT
0
-30
By, nT
0
-30
35
B_z, nT
0
-30
35
|B|, nT
17.5
1500
AE, nT
750
0
0
Dst, nT
-25
-50
DAY 135
DAY 136
DAY 137
DAY 138

Figure 3

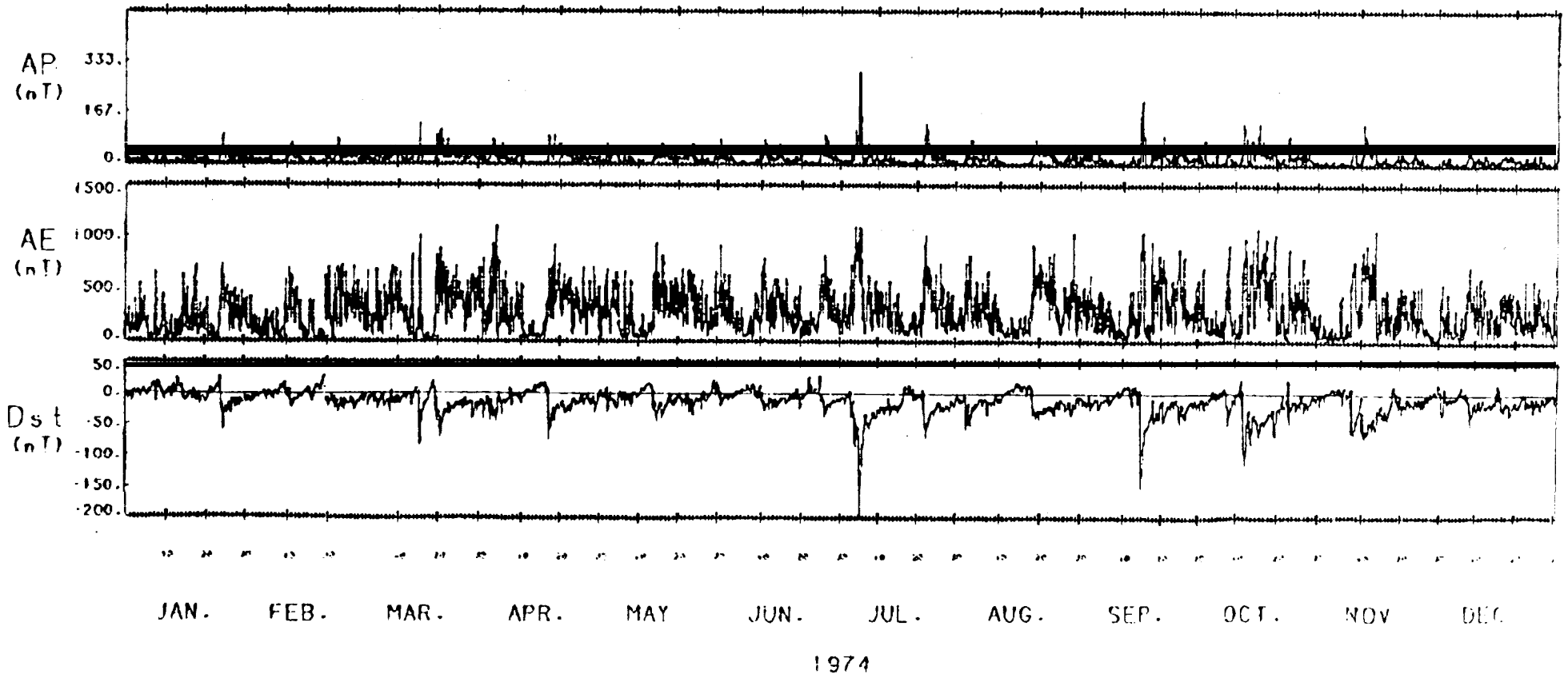
AP
(nT)
333.
167.
0.
AE
(nT)
1500.
1000.
500.
0.
Dst
(nT)
50.
0.
-50.
-100.
-150.
-200.
JAN.
FEB.
MAR.
APR.
MAY
JUN.
JUL.
AUG.
SEP.
OCT.
NOV
DEC
1974

Figure 4

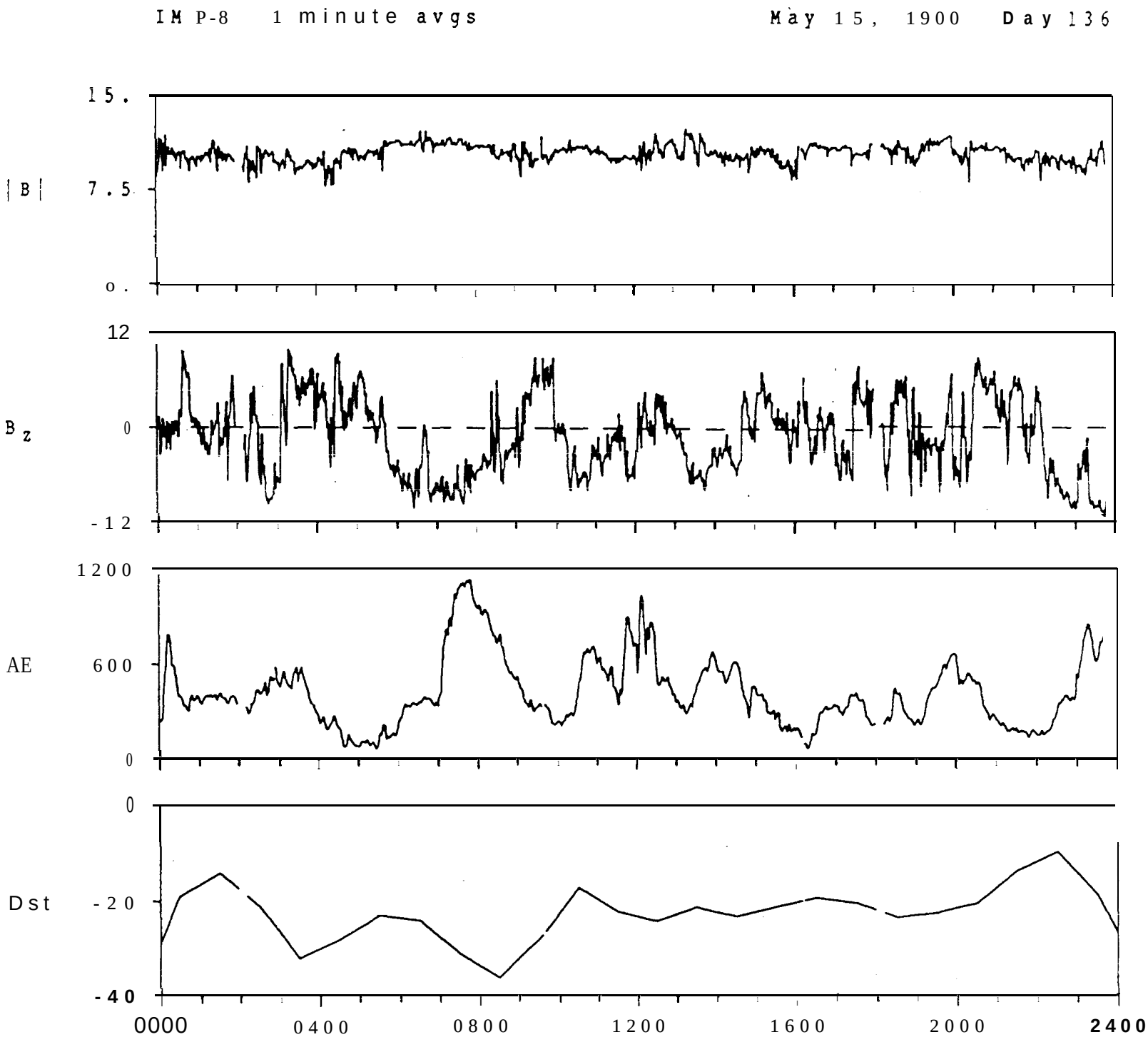
IMP-8 1 minute avgs
May 15, 1900 Day 136
15.
|B| 7.5
0.
12
Bz 0
-12
1200
AE 600
0
0
Dst -20
-40
0000
0400
0800
1200
1600
2000
2400

Figure 5

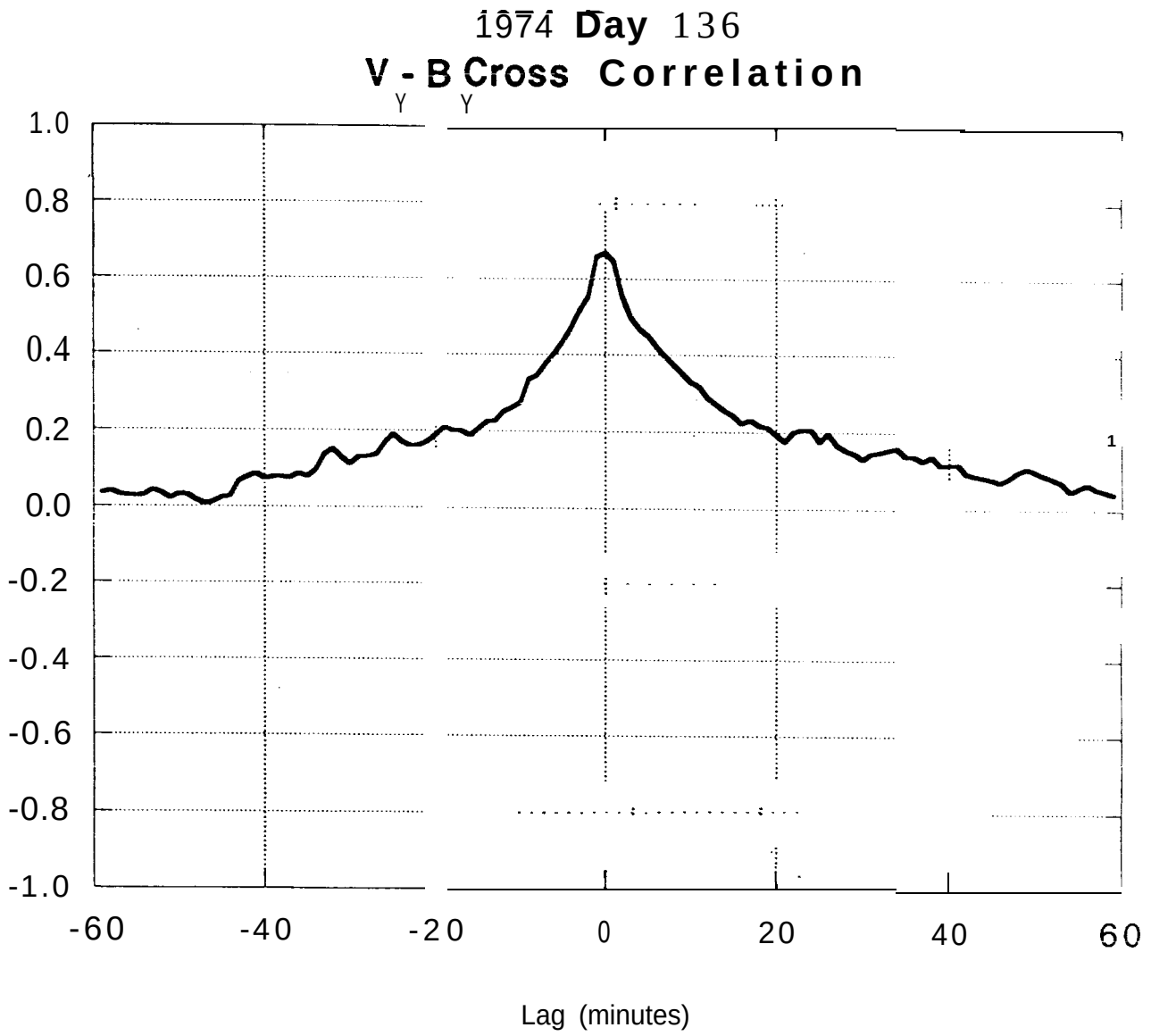
1974 Day 136
V - B Cross Correlation
1.0
0.8
0.6
0.4
0.2
0.0
-0.2
-0.4
-0.6
-0.8
-1.0
-60
-40
-20
0
20
40
60
Lag (minutes)

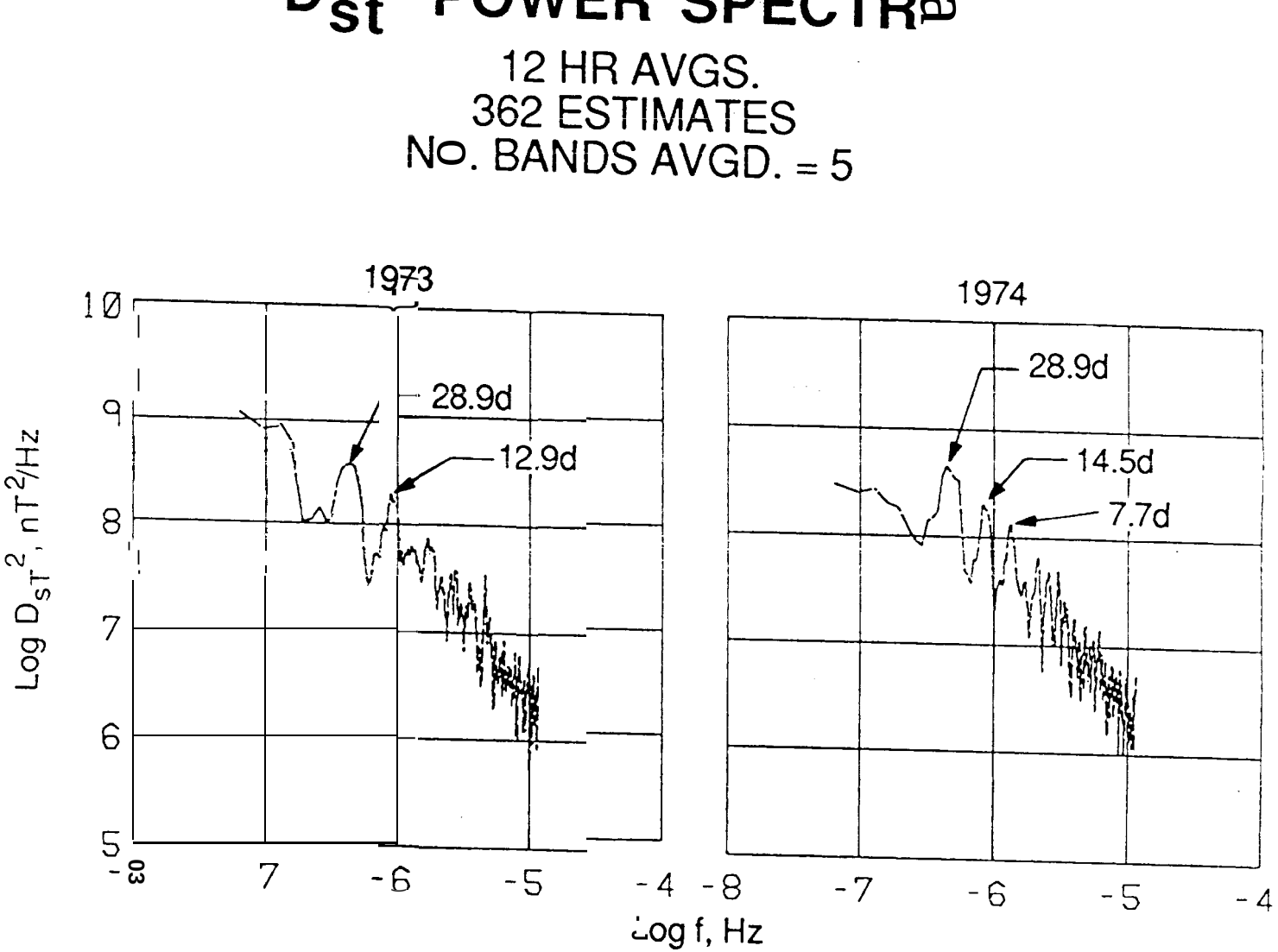
D_{st} POWER SPECTRA
12 HR AVGS.
362 ESTIMATES
No. BANDS AVGD. = 5
1973
1974
28.9d
12.9d
28.9d
14.5d
7.7d
Log D_{sT}^2, nT^2/Hz
Log f, Hz

Figure 7

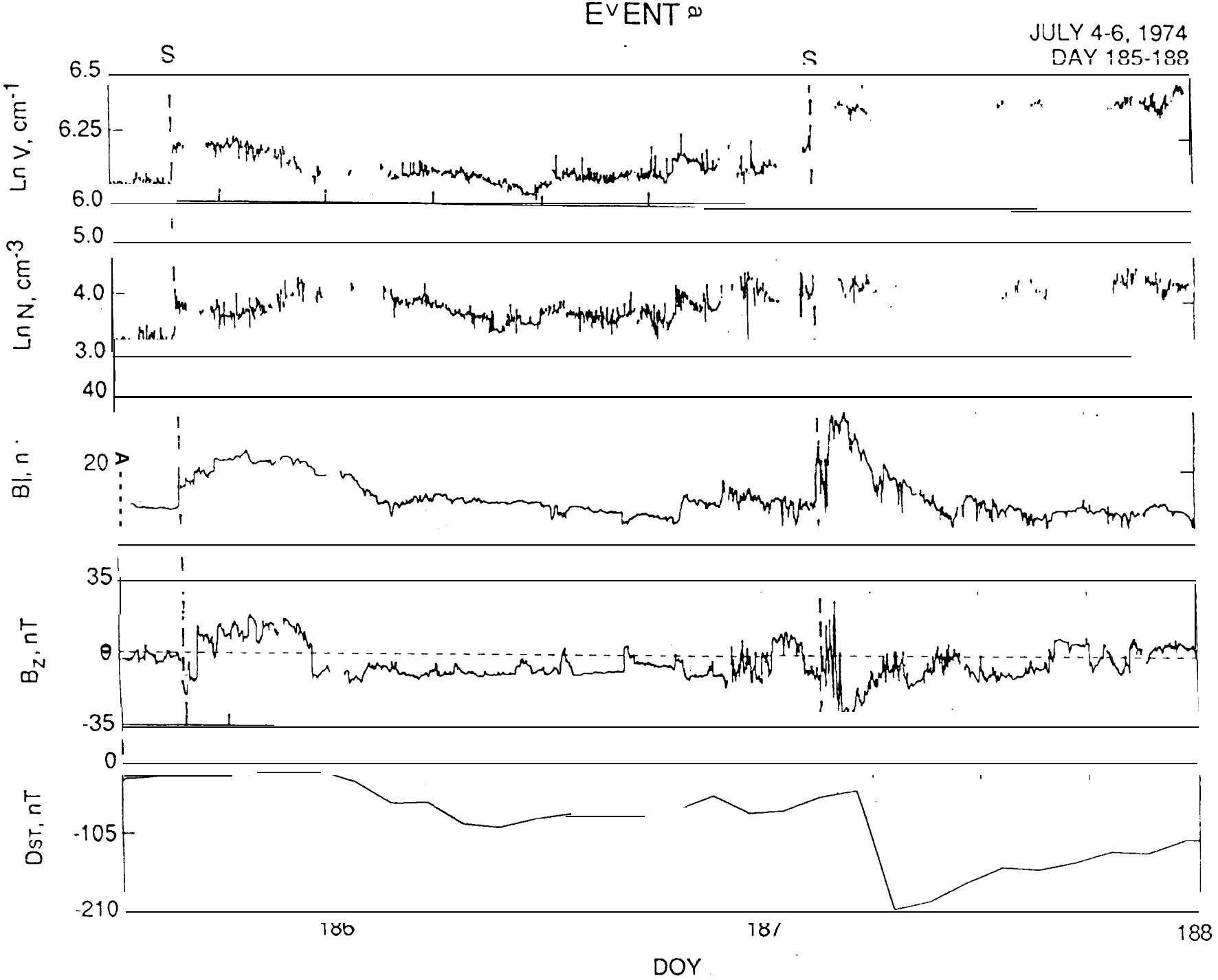
EVENT a
JULY 4-6, 1974
DAY 185-188
S
S
A
Ln V, cm-1
6.5
6.25
6.0
5.0
Ln N, cm-3
4.0
3.0
40
B|, n
20
BZ, nT
35
0
-35
Dst, nT
0
-105
-210
186
187
188
DOY

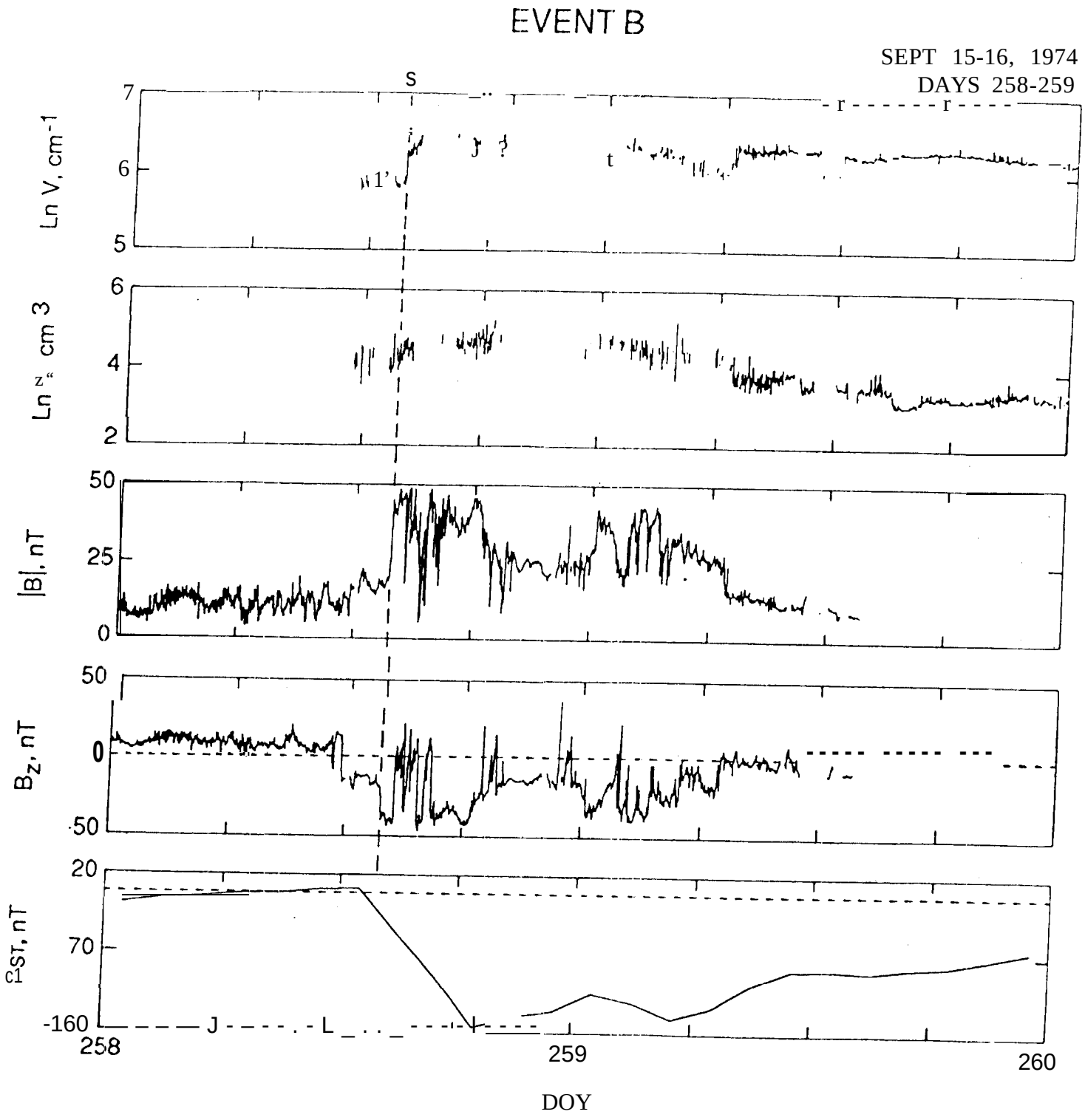
EVENT B
SEPT 15-16, 1974
DAYS 258-259
S
Ln V, cm-1
7
6
5
Ln n, cm 3
6
4
2
|B|, nT
50
25
0
Bz, nT
50
0
-50
σ|B|, nT
20
70
-160
J
L
258
259
260
DOY

Figure 9

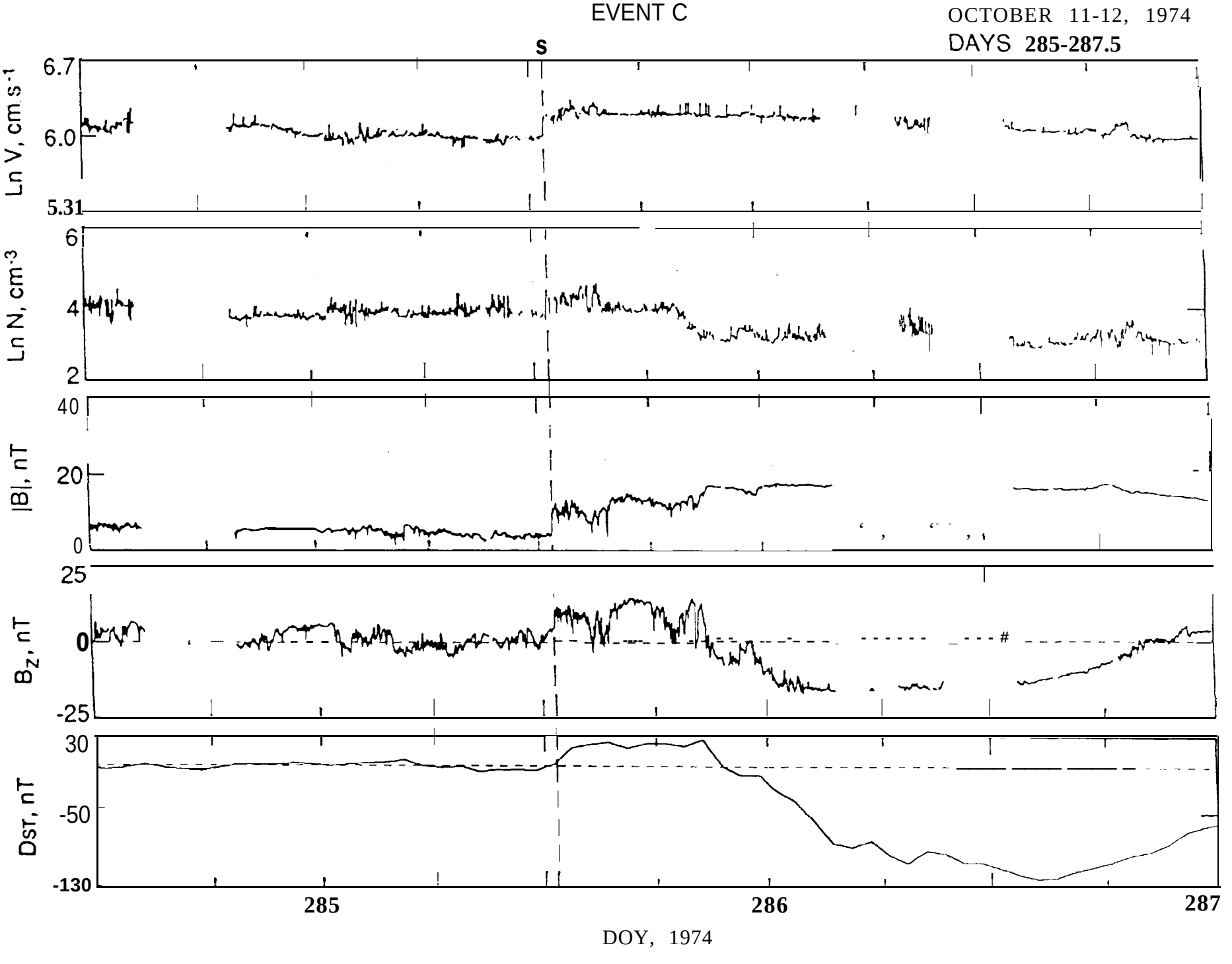
EVENT C
OCTOBER 11-12, 1974
DAYS 285-287.5
S
Ln V, cm s-1
6.7
6.0
5.31
Ln N, cm-3
6
4
2
|B|, nT
40
20
0
Bz, nT
25
0
-25
#
Dst, nT
30
-50
-130
285
286
287
DOY, 1974

Figure 10

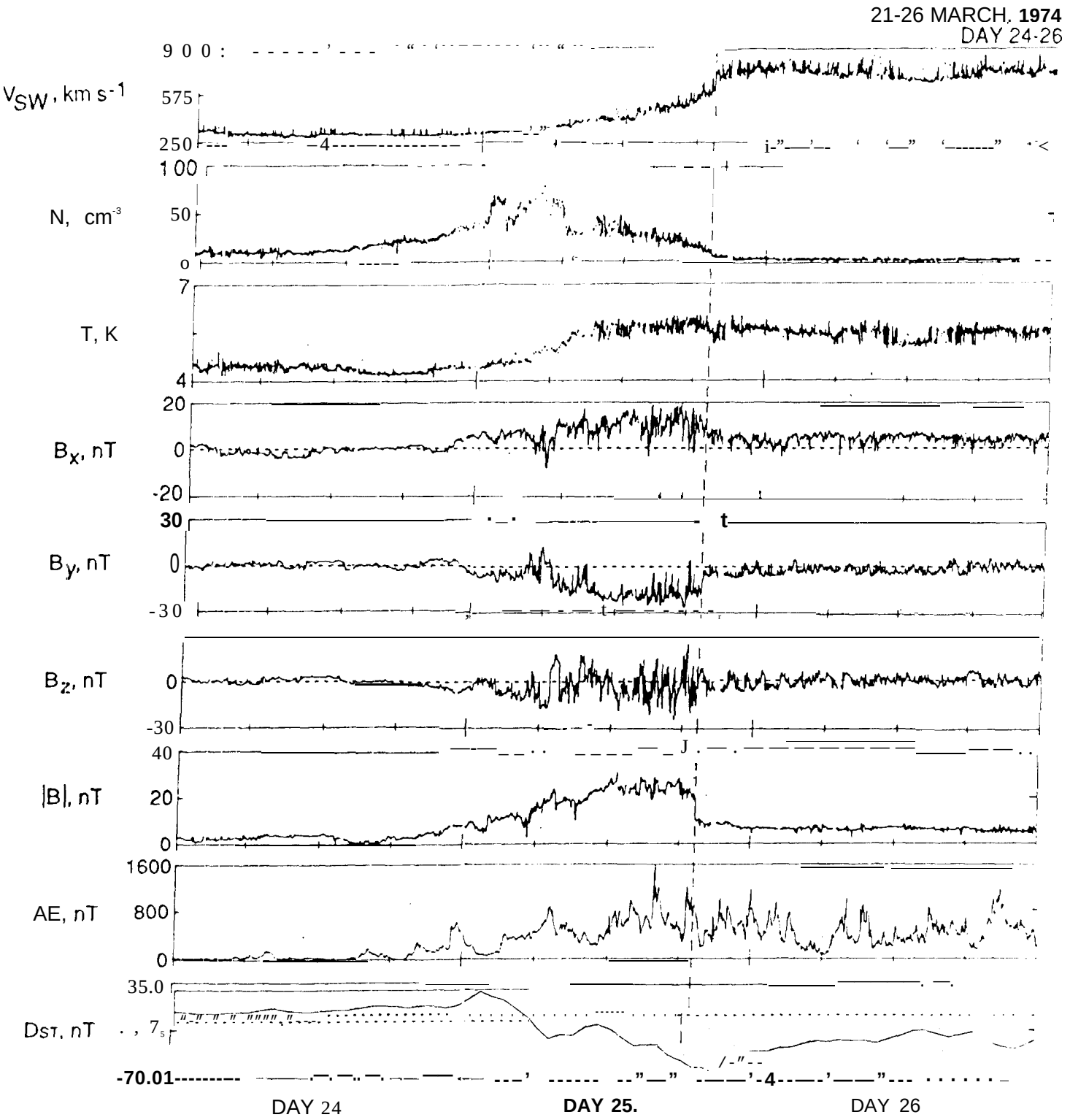
21-26 MARCH, 1974
DAY 24-26
900
V_{SW}, km s^{-1}
575
250
100
N, cm^{-3}
50
0
7
T, K
4
20
B_X, nT
0
-20
30
t
B_Y, nT
0
-30
B_Z, nT
0
-30
40
|B|, nT
20
0
1600
AE, nT
800
0
35.0
Dst, nT
-70.01
DAY 24
DAY 25.
DAY 26

Figure 11

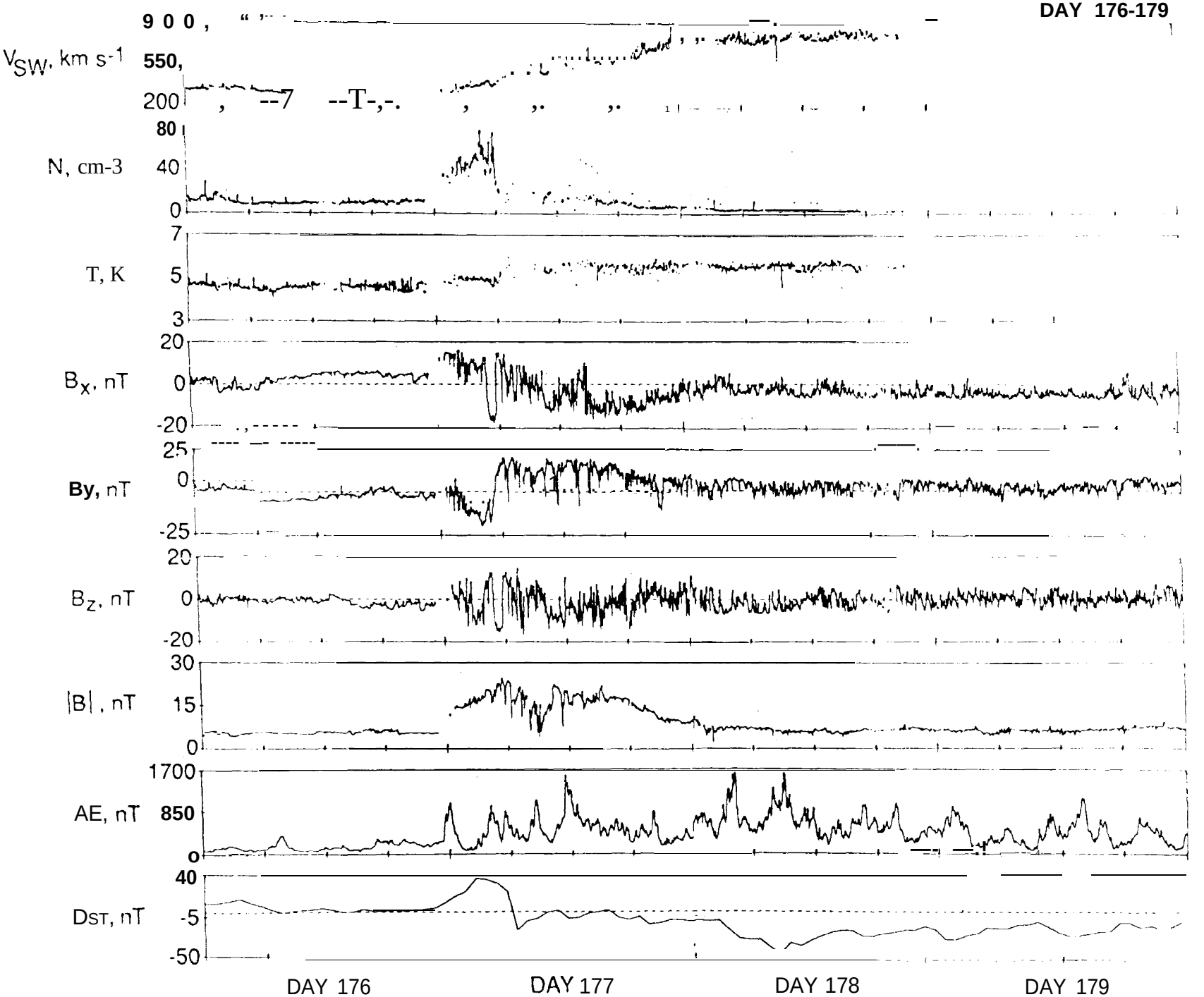
900
V_{SW}, km s-1
550
200
80
N, cm-3
40
0
7
T, K
5
3
20
B_X, nT
0
-20
25
By, nT
0
-25
20
B_Z, nT
0
-20
30
|B|, nT
15
0
1700
AE, nT
850
0
40
DST, nT
-5
-50
DAY 176
DAY 177
DAY 178
DAY 179

Figure 12

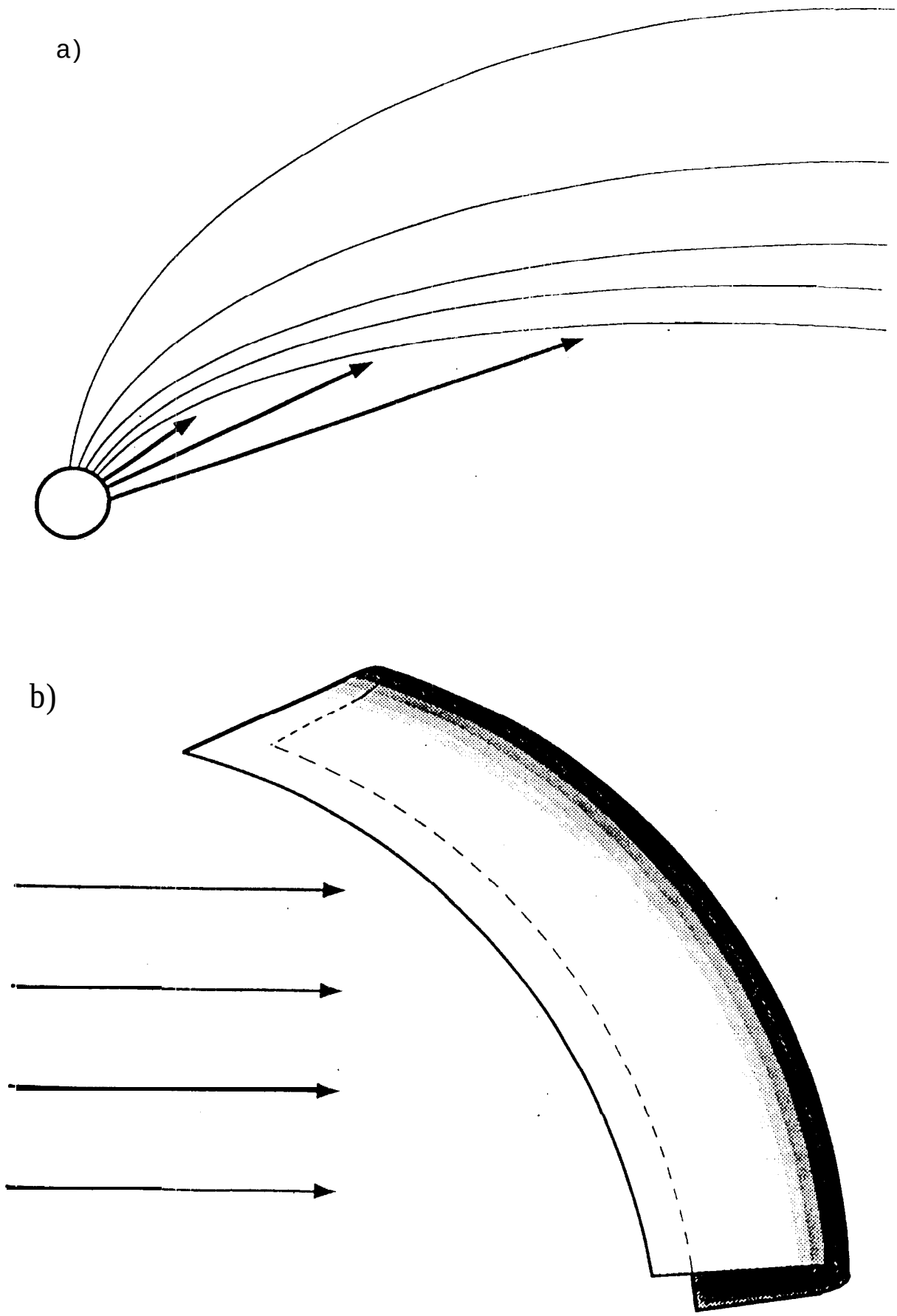

Figure 13

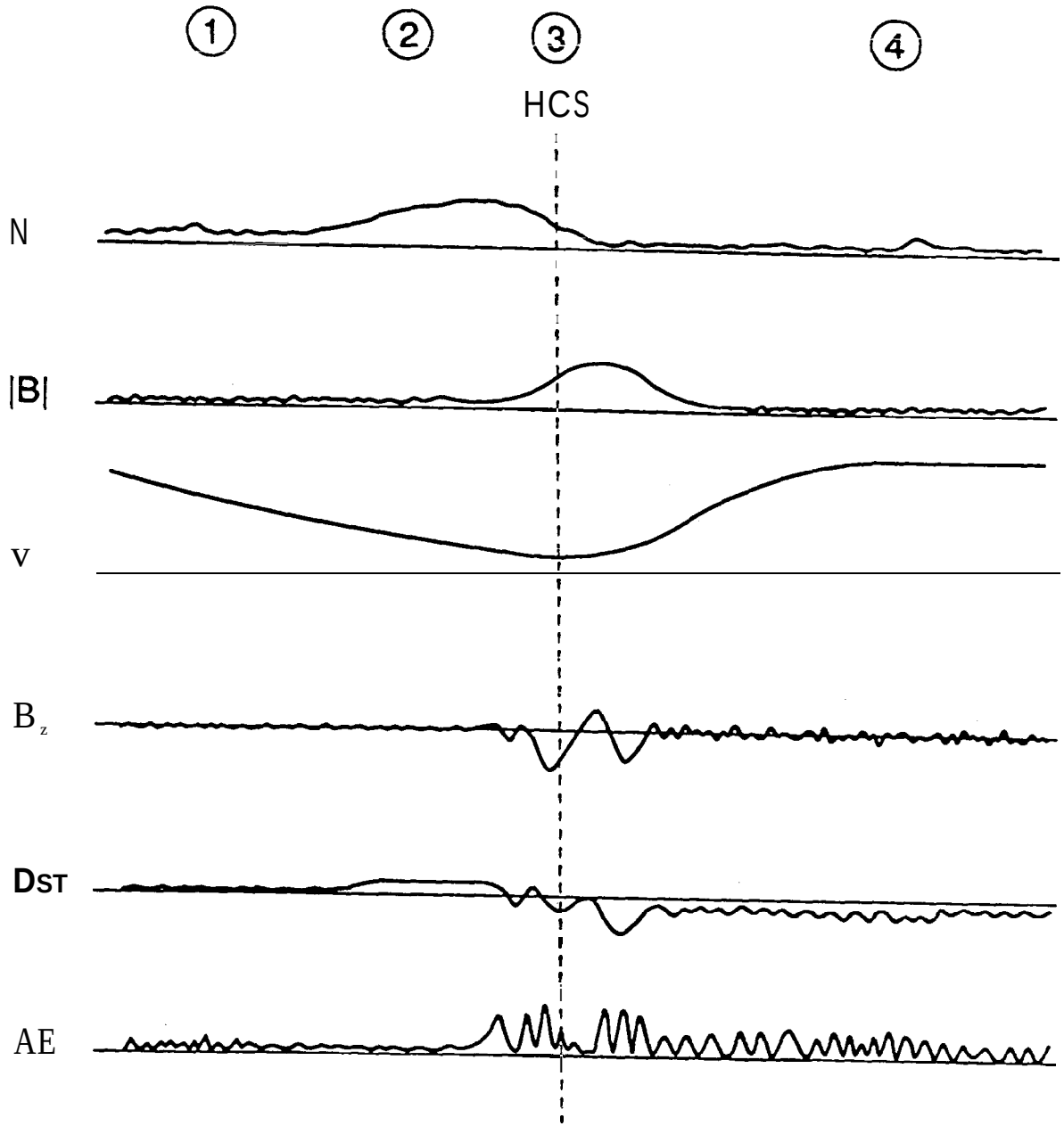

Figure 14